© 2014. Published by The Company of Biologists Ltd | Development (2014) 141, 3529-3539 doi:10.1242/dev.108415

RESEARCH ARTICLE

Simplet/Fam53b is required for Wnt signal transduction by regulating β-catenin nuclear localization

Caghan Kizil[1,*,§], Beate Küchler[1,§], Jia-Jiun Yan[1,§], Günes Özhan[2,‡], Enrico Moro[3], Francesco Argenton[4], Michael Brand[1,2], Gilbert Weidinger[5] and Christopher L. Antos[1,¶]

ABSTRACT

Canonical β-catenin-dependent Wnt signal transduction is important for several biological phenomena, such as cell fate determination, cell proliferation, stem cell maintenance and anterior-posterior axis formation. The hallmark of canonical Wnt signaling is the translocation of β-catenin into the nucleus where it activates gene transcription. However, the mechanisms regulating β-catenin nuclear localization are poorly understood. We show that Simplet/Fam53B (Smp) is required for Wnt signaling by positively regulating β-catenin nuclear localization. In the zebrafish embryo, the loss of *smp* blocks the activity of two β-catenin-dependent reporters and the expression of Wnt target genes, and prevents nuclear accumulation of β-catenin. Conversely, overexpression of *smp* increases β-catenin nuclear localization and transcriptional activity *in vitro* and *in vivo*. Expression of mutant Smp proteins lacking either the nuclear localization signal or the β-catenin interaction domain reveal that the translocation of Smp into the nucleus is essential for β-catenin nuclear localization and Wnt signaling *in vivo*. We also provide evidence that mammalian Smp is involved in regulating β-catenin nuclear localization: the protein colocalizes with β-catenin-dependent gene expression in mouse intestinal crypts; siRNA knockdown of Smp reduces β-catenin nuclear localization and transcriptional activity; human SMP mediates β-catenin transcriptional activity in a dose-dependent manner; and the human SMP protein interacts with human β-catenin primarily in the nucleus. Thus, our findings identify the evolutionary conserved SMP protein as a regulator of β-catenin-dependent Wnt signal transduction.

KEY WORDS: Simplet/Fam53b, Wnt signaling, β-Catenin, Embryogenesis, Nuclear localization, Zebrafish

INTRODUCTION

β-Catenin-dependent Wnt signal transduction is important for several biological phenomena, including anterior-posterior axis formation (Petersen and Reddien, 2009; Cavodeassi, 2013). In the embryo mouse, targeted disruption of Wnt3a results in the loss of caudal somites and the tailbud (Takada et al., 1993). In *Xenopus* embryos, antagonism of Wnt signaling allows the formation of anterior structures at the expense of posterior ones (Leyns et al., 1997; Glinka et al., 1998). This is also true for zebrafish: morpholino knockdown of *wnt8a* results in embryos that predominantly form head but lack posterior structures (Erter et al., 2001; Lekven et al., 2001; Rhinn et al., 2005). Conversely, ectopic activation of Wnt signaling in mouse, *Xenopus* or zebrafish embryos promotes the formation of posterior structures and the loss of anterior ones (Christian and Moon, 1993; Kelly et al., 1995; Popperl et al., 1997; Kiecker and Niehrs, 2001; Rhinn et al., 2005). Thus, Wnt signaling is required for the induction of posterior structures.

β-Catenin-dependent Wnt signal transduction is a multi-step process that consists of several molecular components. It is initiated by secreted Wnt glycoproteins that bind to transmembrane Frizzled receptors (Angers and Moon, 2009). Ligand-receptor interaction induces receptor oligomerization with the low-density lipoprotein receptor-related proteins LRP5 and LRP6 (Angers and Moon, 2009), and this interaction allows LRP5 and LRP6 to bind to the intracellular protein axin. In turn, this complex activates dishevelled, which prevents phosphorylation-mediated degradation of β-catenin, a transcriptional co-factor involved in the activation of genes that are required for specifying posterior structures, e.g. Tbx6 and Cdx4 (Shimizu et al., 2005; Pilon et al., 2006).

The gene *simplet/fam53b* (*smp*) belongs to a family of proteins (Fam53A, Fam53B and Fam53C), the molecular mechanisms of which are unknown. Smp is required for early vertebrate development by regulating progenitor cell proliferation (Thermes et al., 2006), and is also necessary for zebrafish appendage regeneration by regulating cell proliferation and the expression of genes involved in tissue patterning (Kizil et al., 2009). However, it is not understood how Smp is involved in any of these processes, because the molecular mechanisms through which Smp acts have not been determined.

We show that Smp is required for the formation of posterior structures during zebrafish embryogenesis, and that the *smp* knockdown phenotype is associated with the abrupt inactivation of β-catenin-dependent Wnt signaling at late gastrulation due to the loss of nuclear β-catenin. We also show that the Smp protein interacts with β-catenin and that loss of the nuclear localization signal in Smp inhibits β-catenin-dependent Wnt signaling by preventing nuclear localization of β-catenin. Furthermore, subcellular fractionation experiments indicate that Smp and β-catenin interact in the nucleus, and fluorescence recovery after photobleaching experiments suggest that Smp is involved in retaining β-catenin in the nucleus. Thus, we identify a previously unknown regulator of β-catenin-dependent Wnt signaling.

[1]DFG-Center for Regenerative Therapies Dresden (CRTD), Technische Universität Dresden, Fetscherstrasse 105, Dresden 01307, Germany. [2]Biotechnology Center, Technische Universität Dresden, Tatzberg 47-49, Dresden 01307, Germany. [3]Department of Molecular Medicine, University of Padua, Via U. Bassi 58/B, Padua 25131, Italy. [4]Department of Biology, University of Padua, Via U. Bassi 58/B, Padua 35131, Italy. [5]Institute for Biochemistry and Molecular Biology, Ulm University, Ulm 89081, Germany.
*Present address: German Center for Neurodegenerative Diseases (DZNE) Dresden within Helmholtz Association, Arnoldstrasse 18, Dresden 01307, Germany. ‡Present address: Advanced Biomedical Research Center, Dokuz Eylül University Health Campus, Incrialti-Izmir, Turkey.
§These authors contributed equally to this work

¶Author for correspondence (christopher.antos@crt-dresden.de)

Received 27 January 2014; Accepted 4 July 2014

Development (2014) 141, 3529-3539 doi:10.1242/dev.108415

RESULTS

smp knockdown results in loss of posterior structures and β-catenin-dependent gene transcription

Previous work has shown that Smp is required for early Medaka embryogenesis and zebrafish fin regeneration (Thermes et al., 2006; Kizil et al., 2009), but the molecular mechanisms through which it functions during these processes are unknown. Smp shares some similarity within two domains with two other genes (Fam53A and Fam53C) (supplementary material Fig. S1A); the two conserved domains in these proteins have no clear similarity to any known protein domain. *smp* is present as a transcript (Fig. 1A-E) and protein (supplementary material Fig. S1B-G) during early zebrafish embryogenesis. To elucidate how *smp* functions, we performed morpholino knockdown in the zebrafish embryo. Compared with mismatch-injected (MM) control embryos (Fig. 1F), the knockdown of *smp* with previously characterized translation (ATG) or splice-blocking morpholinos (Kizil et al., 2009) produced axial defects (Fig. 1G,H; supplementary material Fig. S2A,B).

Loss of zygotic β-catenin-dependent Wnt signaling also results in axial defects (Lekven et al., 2001; Agathon et al., 2003; Shimizu et al., 2005; Petersen and Reddien, 2009). We therefore tested whether loss of *smp* affected the activity of Wnt signaling-dependent transgenic zebrafish reporter lines: Tg(7xTCF-XLa.Siam:nlsmCherry)^{ia5} [hereafter Tg(7xTCF:mCherry)] and Tg(Top:dGFP) (Dorsky et al., 2002; Moro et al., 2012). Although *smp* knockdown did not affect Tg(7xTCF:mCherry) reporter expression at 85% epiboly (Fig. 1I,J), at 95% epiboly and later stages the reporter activity observed in mismatch controls (Fig. 1K,M) was nearly abolished in the *smp* antisense (AS) morphants (Fig. 1L,N). Co-injecting *smp* mRNA with the antisense morpholino targeting the splice site restored the reporter activity (supplementary material Fig. S2C-F) and rescued the axial defects (supplementary material Fig. S2G-J), indicating that the loss of reporter activity is specifically due to the loss of Smp function (Kizil et al., 2009). Similar results were obtained using the transgenic Top:dGFP Wnt-reporter line (Fig. 1O-R). *cdx4*, *tbx6* and *gbx1* are β-catenin-dependent Wnt-regulated genes that are required for axial patterning (Chapman and Papaioannou, 1998; Lekven et al., 2001; White et al., 2003; Rhinn et al., 2005, 2009; Shimizu et al., 2005; Pilon et al., 2006). Compared with controls (Fig. 1S,U,W,Y,AA), *smp* morphants showed significant downregulation of these genes (Fig. 1V,Z,BB), demonstrating that *smp* is required for Wnt-dependent gene expression in the embryo. The emergence of the smp morphant phenotype is likely due to a maternally loaded Smp protein (supplementary material Fig. S2O,P), as detected using an antibody for the zebrafish Smp protein (supplementary material Fig. S2K-M′).

BMP, Nodal, FGF and retinoic acid signaling pathways are also required for axial patterning of the embryo (Schier, 2001; Schier and Talbot, 2005; Rhinn et al., 2006), and BMP, Nodal and FGF appear unaffected during gastrulation of the morphants (supplementary material Fig. S3). Although the retinoic acid-synthesizing enzyme *aldh1a2* (*raldh2*) was unaffected (supplementary material Fig. S4A-B′), *smp* knockdown caused ectopic expression of the retinoic acid-degrading enzyme *cyp26a1* at tailbud stage (supplementary material Fig. S4C-F). This broader expression was subsequent to the loss in activity of the β-catenin-dependent reporter (supplementary material Fig. S4G,H), and similar misregulation was induced by Dkk1 overexpression (supplementary material Fig. S4I,J), indicating that the altered expression of *cyp26a1* in the *smp* morphants is a downstream consequence of Wnt inhibition.

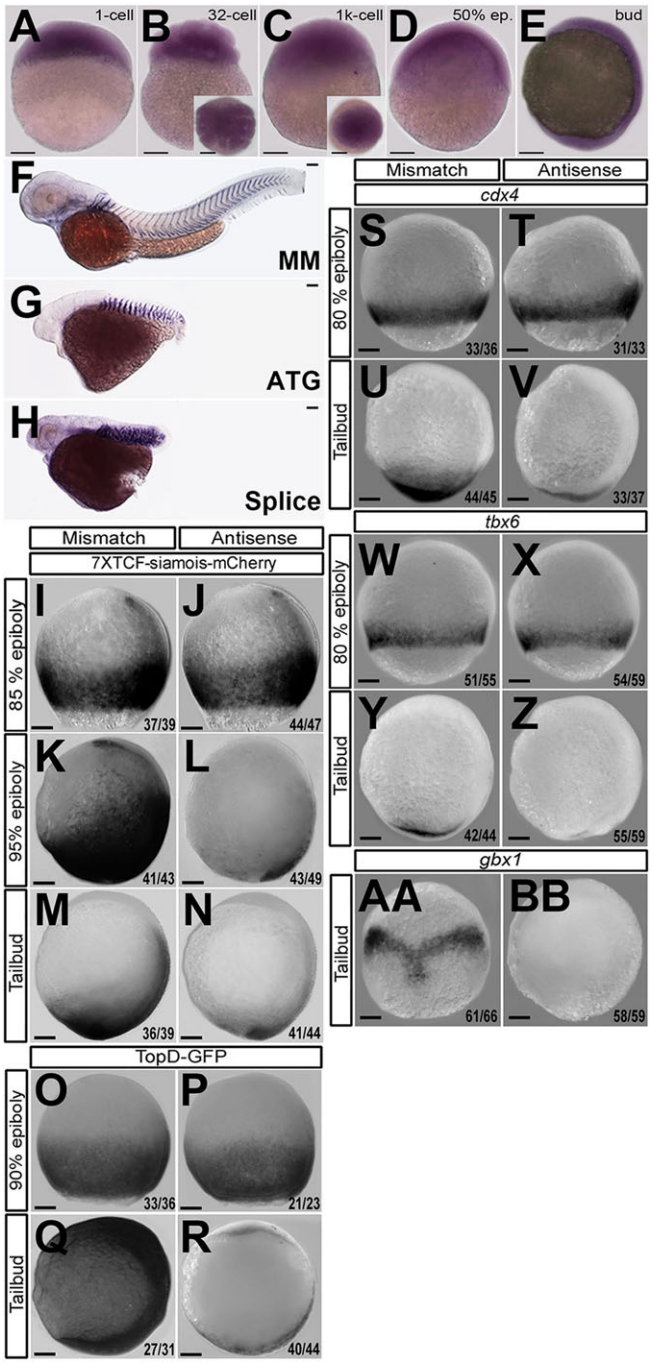

Fig. 1. Loss of *smp* causes Wnt-related developmental phenotype and loss of Wnt-dependent gene expression. (A) *smp* mRNA (dark purple) in the single-cell embryo. (B,C) The *smp* transcript in 32-cell embryo (B) and in 1000-cell embryo (C). Expression remains ubiquitous at 50% epiboly (D) and at tailbud (lateral view) stage (E). (F) Control embryo (MM) 24 h post-fertilization (hpf) after injection with mismatch *smp* morpholino at the one-cell stage. *In situ* hybridization with a *xirp2* probe highlights somatic muscle boundaries. (G,H) Injection of antisense morpholino to the start (ATG) site (G) or first intron-exon (splice) boundary (H) of *smp* in 24 hpf embryos. Activation of 7xTCF:mCherry in mismatch control embryos (I,K,M) compared with *smp* morphants (J,L,N). Activity of Top:dGFP in control embryos (O,Q) compared with *smp* morphants (P,R). *cdx4* expression at indicated stages in mismatch controls (S,U) and in *smp* morphants (T,V). Expression of *tbx6* at indicated stages in controls (W,Y) and *smp* morphants (X,Z). Expression of *gbx1* at tailbud stage in controls (AA) and *smp* morphants (BB). Numbers in lower right corners of the panels indicate the number of embryos with the depicted expression pattern/the total number of animals. Scale bars: 100 µm.

Development (2014) 141, 3529-3539 doi:10.1242/dev.108415

Subsets of Wnt ligands activate β-catenin-independent planar cell polarity (PCP) signaling, which regulates convergence-extension movements during vertebrate gastrulation (Du et al., 1995; Heisenberg et al., 2000; Tada and Smith, 2000; Kilian et al., 2003; Roszko et al., 2009). We therefore examined the expression of these ligands, the cell contribution to the embryo during PCP-dependent convergence extension and the gene expression associated with PCP signaling. Comparisons between controls and morphants in these experiments indicated no apparent abnormalities normally attributed to defective Wnt-PCP signaling in *smp* morphants (supplementary material Fig. S5). Using markers for neuroectoderm, endoderm, paraxial mesoderm and somatic mesoderm specification, we observed similar expression patterns in control and *smp* knockdown embryos (supplementary material Fig. S6) despite the expected a reduction of proliferating cells in the morphants (supplementary material Fig. S6I-N) (Thermes et al., 2006). However, we observed a slight temporary thickening in the expression pattern of genes transcribed in the axial mesoderm, indicating a short-term (possibly indirect) effect on early axial development before the loss of β-catenin-mediated signaling (supplementary material Fig. S6O-W). Although treatment with hydroxyurea (HU) and aphidicolin (AC) significantly reduced cell proliferation, it did not inhibit β-catenin-dependent Tg(7XTCF:mCherry) reporter activity (supplementary material Fig. S7). Apoptosis was not significantly altered in *smp* morphants (supplementary material Fig. S8A,B), and preventing apoptosis by *p53* knockdown (supplementary material Fig. S8C) did not prevent the loss of Wnt reporter activity (supplementary material Fig. S8D-F). Together, these results suggest that the loss of Wnt signaling is not due to defects in early germ layer formation or to perturbed cell proliferation or death.

Smp is required for β-catenin-dependent signaling by regulating its nuclear localization

We next asked whether *smp* acts up- or downstream of β-catenin in the Wnt signaling pathway. Compared with control (Fig. 2A) and *smp* morphants (Fig. 2B), overexpression of β-catenin expanded the activity of the Tg(7xTCF:mCherry) reporter (Fig. 2C). Interestingly, *smp* knockdown suppressed the β-catenin-mediated expansion of the reporter (Fig. 2D). By contrast, *smp* knockdown did not suppress the activation of the reporter by a β-catenin-independent constitutive active *lef1* construct (*lef1* fused to the VP16 transactivation domain, *lef1*-VP16) (Aoki et al., 1999; Vleminckx et al., 1999) (Fig. 2E,F). In addition, we found that the Wnt ligands required for axis formation are expressed and that Wnt receptor complex activation in unaffected, as evidenced by similar Lrp6 phosphorylation levels in the morphants as in MM controls (supplementary material Fig. S9). These results indicate that *smp* is involved in Wnt signal transduction by regulating β-catenin activity.

β-Catenin transduces Wnt signaling by accumulating in the cytoplasm and translocating to the nucleus (Grigoryan et al., 2008). Immunohistochemistry (IHC) for β-catenin in MM-control embryos showed β-catenin at the plasma membrane and in the nuclei of marginal deep cells (Fig. 2G,H). However, although β-catenin was localized to the plasma membrane (Fig. 2I), it was absent in the nuclei of *smp* morphants (Fig. 2J). Subcellular fractionation experiments also showed that compared with the levels of β-catenin in the nuclear fraction of MM-control embryos, β-catenin was significantly reduced in the nuclear fraction of *smp* morphants and was comparatively higher in the cytoplasmic fraction (Fig. 2K, supplementary material Fig. S10A). The overall levels of β-catenin in the morphants remained unchanged (Fig. 2K), indicating that *smp* is required for β-catenin nuclear localization and not for its stabilization, and that the loss of *smp* results in a shift from nuclear to cytoplasmic distribution of β-catenin.

The dependence of β-catenin nuclear localization on *smp* suggests that the proteins colocalize in the nucleus. Immunohistochemistry with antibodies (supplementary material Fig. S10B,C) against endogenous zebrafish Smp (Fig. 2L) and β-catenin (Fig. 2M) in the dorsal marginal cells showed nuclear co-staining of both proteins (Fig. 2N, white arrowheads). However, several Smp-positive nuclei lacked β-catenin (Fig. 2M, white arrows), indicating that while β-catenin requires Smp for its nuclear localization, the nuclear localization of Smp does not require β-catenin.

We next addressed the ability of Smp to activate β-catenin-dependent Wnt signaling. Because transfection experiments showed that Smp alone failed to activate the pBAR reporter (supplementary material Fig. S11A), Smp appeared to be unable to promote Wnt signaling alone. We compared the distribution of the phenotypic classes from overexpression of *wnt8* with GFP (Fig. 2O) and of *smp* with *wnt8*. We observed that *smp* exacerbated the severity of *wnt8*-induced phenotypes in zebrafish (Fig. 2P). Likewise, *smp* enhanced the activation of the β-catenin-dependent reporter pBAR in HEK293T cells by *wnt8* (Fig. 2Q) as well as by other members of the Wnt signaling cascade (supplementary material Fig. S11B). Furthermore, in zebrafish PAC2 cells, Smp synergized with β-catenin in pBAR activation in a dose-dependent manner (supplementary material Fig. S11C). These results indicate that *smp* mediates β-catenin-dependent Wnt signal transduction.

We next assessed whether the enhancement of β-catenin-dependent Wnt signaling by *smp* is associated with an increase in the nuclear localization of β-catenin. Immunohistochemical staining of embryos overexpressing Smp-GFP showed nuclear localization of the Smp-GFP (Fig. 2S). Whereas endogenous β-catenin was primarily localized at the cell membrane with faint staining in the nucleus of controls (Fig. 2T), overexpression of Smp-GFP increased nuclear β-catenin (Fig. 2U). Smp-GFP and β-catenin co-stains showed that cells with Smp in the nucleus contained nuclear-localized β-catenin (Fig. 2Y). We quantified the distribution of both proteins and observed that when β-catenin was nuclear, Smp was nuclear (>99%) (Fig. 2Z). However, cells lacking nuclear β-catenin displayed nuclear localization of Smp in ~85% of cells counted (Fig. 2AA), suggesting that Smp nuclear localization is not regulated by Wnt signaling. To examine whether Smp transcription is regulated by Wnt signaling, we used transgenic fish lines that activate or inhibit Wnt signaling and found no change in *smp* expression *in vivo* (supplementary material Fig. S12A-D). Likewise, there was no change in subcellular distribution of the protein in cells cultured with Wnt-conditioned medium *in vitro* (supplementary material Fig. S12E-J). These data associate the nuclear localization of β-catenin with nuclear Smp and argue that Smp itself does not require β-catenin to localize to the nucleus.

Removal of the nuclear localization signal in Smp prevents β-catenin nuclear localization and inhibits Wnt signaling

Smp protein contains a candidate nuclear localization signal (NLS), which could be instrumental in mediating β-catenin nuclear accumulation (Fig. 3A). We therefore tested its importance by generating a NLS mutant that still interacts with β-catenin (Fig. 3A; supplementary material Fig. S13A). Overexpression of the GFP-tagged full-length Smp (Smp-FL-GFP) showed predominant nuclear localization in the dorsal region in zebrafish embryos (Fig. 3B), whereas a Smp deletion construct lacking the NLS (Smp-ΔNLS-GFP) showed a completely cytoplasmic distribution

Development (2014) 141, 3529-3539 doi:10.1242/dev.108415

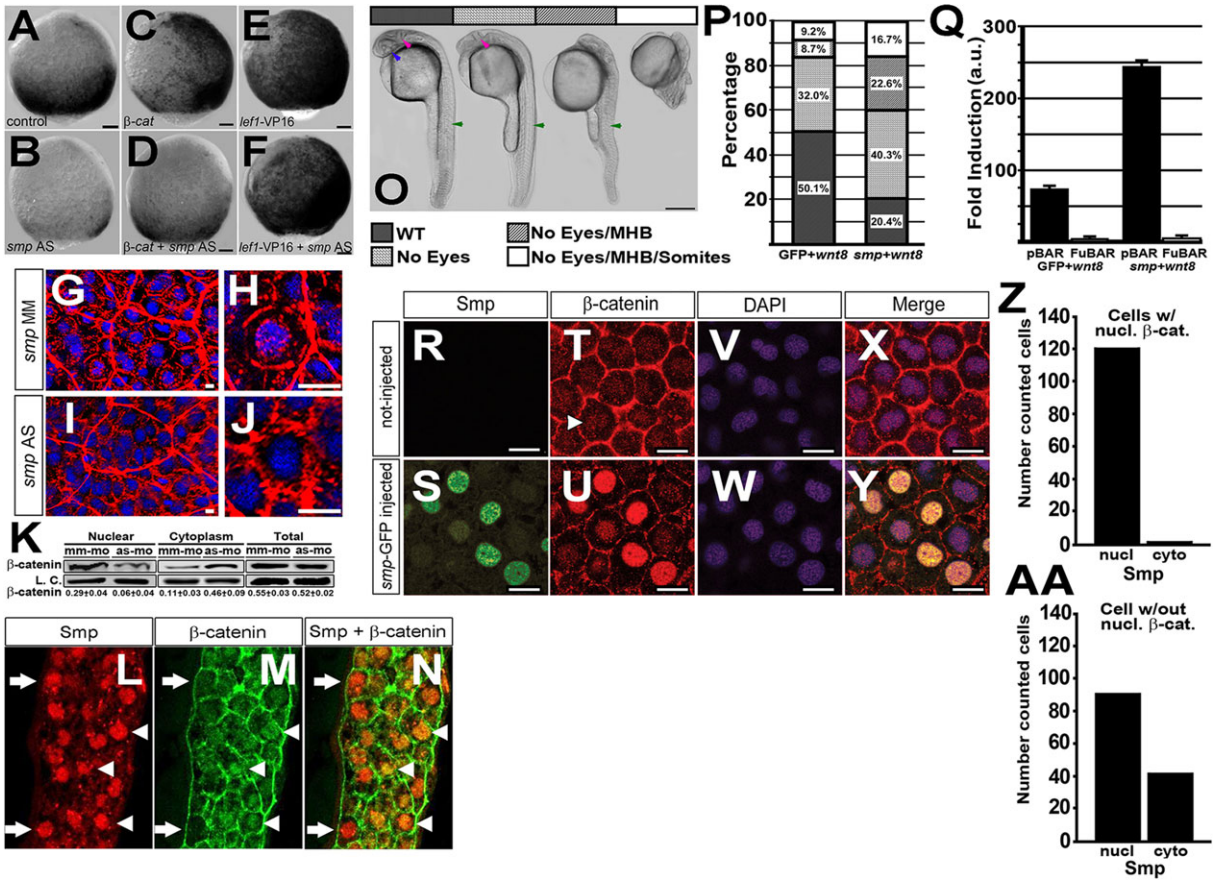

Fig. 2. Smp regulates β-catenin nuclear localization. (A) Activity of the 7xTCF:mCherry transgene at 95% epiboly after mismatch morpholino injection, (B) knockdown of *smp*, (C) overexpression of β-catenin in mismatch controls and (D) overexpression of β-catenin in *smp* morphants. (E) Activity of the 7xTCF:mCherry transgene at 95% epiboly after overexpression of *lef1*-VP16 in mismatch controls and (F) overexpression of *lef1*-VP16 in *smp* morphants. (G,H) Immunohistochemistry staining for β-catenin (red) and staining of nuclei with DAPI (blue) in mismatch control and (I,J) *smp* morphants. (K) Western blots for β-catenin in nuclear and cytoplasmic lysates from mismatch-morpholino controls (mm-mo) and *smp* morphants (as-mo). Total amount of β-catenin levels in the cells was unaltered by the *smp* knockdown. Loading controls were γ-tubulin for the cytoplasmic fraction and H2A for the nuclear fraction. (L) Immunohistochemistry staining for zebrafish Smp shows positive nuclei in the marginal zone where Wnt signaling is active. (M) Immunohistochemistry staining for β-catenin shows localization at the plasma membrane and in distinct nuclei (white arrowheads). (N) Merged stainings show colocalization of Smp and β-catenin in nuclei (white arrowheads) and cells with Smp in nuclei lacking β-catenin (white arrows). (O) Overexpression of *wnt8* during zebrafish development produces phenotype classes that affect normal development of eyes (blue arrow); the midbrain-hindbrain boundary (pink arrow); and the somites and posterior structures (green arrows). (P) Percentage occurrence of phenotypic classes produced by overexpression of *wnt8* alone or overexpression of *wnt8* with *smp*. (Q) Results of luciferase assays of either the pBAR reporter (β-catenin binding sites) or the pFuBAR reporter (mutated β-catenin sites) for Wnt activity in HEK293T cells. (R) Uninjected controls. (S) GFP localization in the nuclei of embryos injected with mRNA encoding Smp-GFP. (T) β-Catenin localization in the dorsal region of control embryos. (U) β-Catenin localization in Smp-GFP-injected embryos. (V,W) DAPI staining labels nuclei. (X,Y) Merged fluorescence for β-catenin, GFP and DAPI. (Z) The number of β-catenin-positive cells with Smp in the nucleus or in the cytoplasm. (AA) The subcellular distribution of Smp in cells lacking β-catenin nuclear staining. Scale bars: 10 μm in A-G,I,L-N; 1 μm in H,J; 300 μm in O; 10 μm in R-Y. All experiments were performed at least three times. Data represent the mean; error bars indicate s.d.

(Fig. 3C). To assess whether β-catenin nuclear localization is perturbed by the cytoplasmic localization of Smp, we compared the subcellular distribution of endogenous β-catenin in the presence either of Smp-FL-GFP or of Smp-ΔNLS-GFP. Compared with β-catenin nuclear localization in Smp-FL-GFP-expressing cells (Fig. 3D,F), the Smp-ΔNLS-GFP-positive cells showed a lack of nuclear β-catenin (Fig. 3E,G). These results indicate that Smp nuclear localization is required for the nuclear accumulation of both Smp and β-catenin.

We next tested whether the Smp-ΔNLS can act as a dominant-negative that interferes with the activation of the Tg(7xTCF:mCherry) reporter and found that, compared with overexpression of GFP (Fig. 3H) or of Smp-FL-GFP (Fig. 3I), overexpression of Smp-ΔNLS-GFP significantly reduced the activation of the reporter (Fig. 3J). Furthermore, we observed posterior truncations similar to those in the *smp* morphants and reminiscent of Wnt loss-of-function phenotypes for Smp-ΔNLS-GFP injected embryos (Fig. 3M,P) when compared with the overexpression of GFP (Fig. 3K,N) and Smp-FL-GFP (Fig. 3L,O). We also tested whether Smp-ΔNLS-GFP is able to antagonize enhanced Wnt signaling. Compared with GFP-expressing controls (Fig. 3Q,Q′), transgenic embryos expressing Wnt8-GFP displayed loss of anterior structures (Fig. 3R,R′). However, injection of Smp-ΔNLS-GFP rescued the Wnt8-induced phenotypes (Fig. 3S,S′), and the extent of rescue was directly associated with the amount of injected Smp-ΔNLS mRNA (Fig. 3T). We also assessed the effects of Smp-ΔNLS on the transcriptional activity of β-catenin. Injection of a stabilized β-catenin (Fig. 3V; supplementary material Fig. S13) or β-catenin with full-length Smp (Fig. 3W; supplementary material Fig. S13) showed increased reporter activity in Tg(7xTCF:mCherry) embryos compared with controls (Fig. 3U; supplementary material

Development (2014) 141, 3529-3539 doi:10.1242/dev.108415

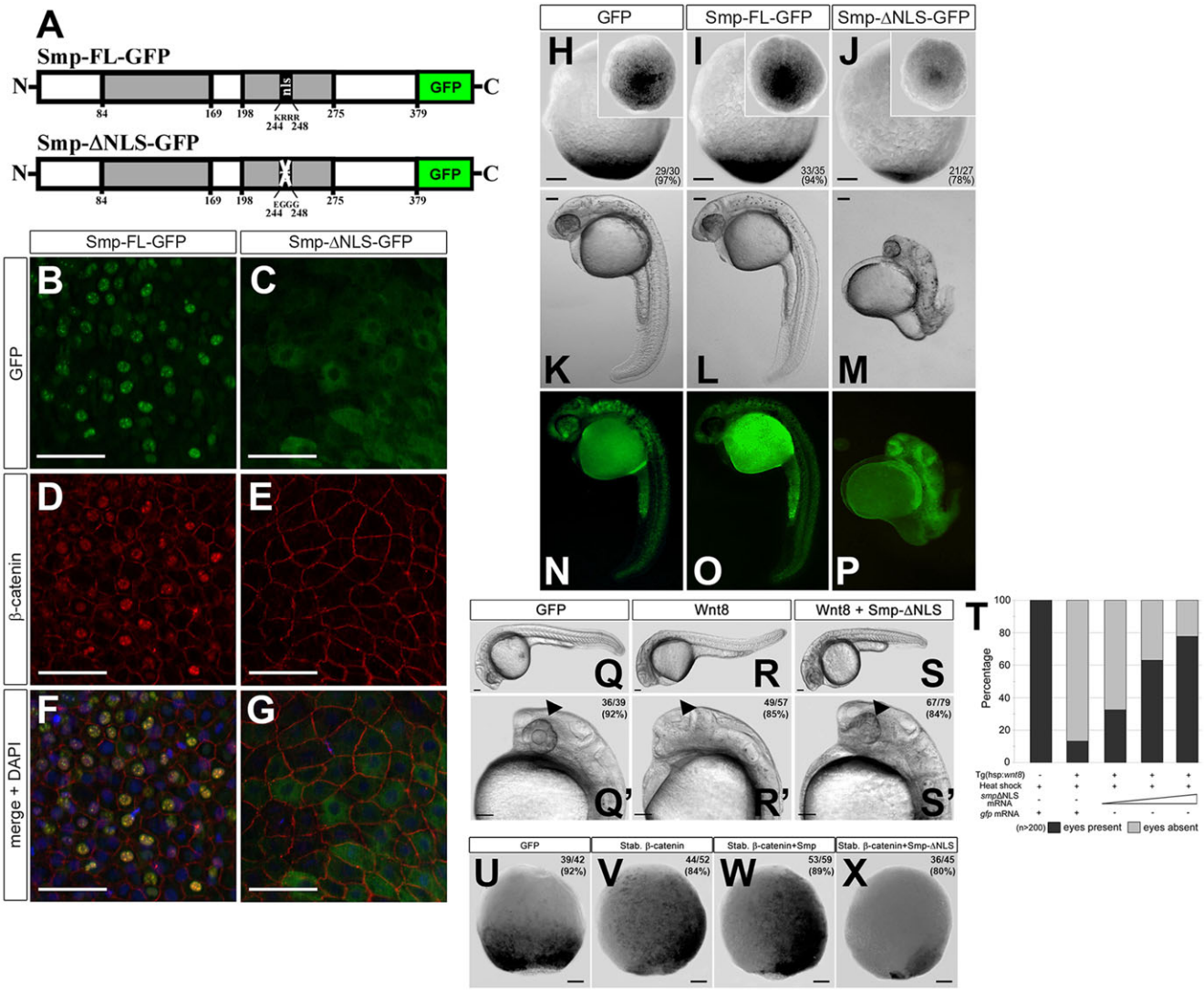

Fig. 3. Nuclear localization of β-catenin requires the Smp nuclear localization signal. (A) The domain structure of Smp. The two grey boxes indicate regions of significant conservation among vertebrates. The numbers indicate the position of the amino acids. 'nls' identifies the nuclear localization signal KRRR. Substitution of these amino acids with EGGG ablates the nuclear localization signal (white cross). (B) Overexpression of Smp-GFP in fish embryos. (C) Deletion of the nuclear localization signal in Smp-GFP. (D) Co-staining for β-catenin in Smp-GFP-injected embryo. (E) Co-staining for β-catenin in Smp-ΔNLS-GFP-injected embryo. (F) Overlay of Smp-GFP and β-catenin immunostainings in Smp-GFP-injected embryo. (G) Overlay of Smp-GFP and β-catenin immunostaining in Smp-ΔNLS-GFP-injected embryo. (H-J) Overexpression of GFP (H), Smp-FL (I) or Smp-ΔNLS (J) in the Tg(7xTCF:mCherry) embryos at tailbud stage. (K) Overexpression of GFP in a 24 hpf embryos. (L) Overexpression of Smp-GFP in 24 hpf embryo. (M) Overexpression of Smp-ΔNLS-GFP in 24 dpf embryo. (N-P) Expression of each GFP-fused construct in the injected embryos. (Q,Q′) Control-injected transgenic embryos at 24 hpf. (R,R′) Transgenic overexpression of *wnt8*. (S,S′) Injection of *smp*-ΔNLS into embryos transgenically overexpressing *wnt8*. Arrowheads indicate the expected location of the developing eye. (T) Graph shows a direct correlation between the rescue from the wnt8-overexpression posteriorization phenotype and the amount of *smp*-ΔNLS mRNA injected. Data are the average percent. (U) Control-injected Tg(7xTCF:mCherry) embryos. (V) Injection of mRNA encoding stabilized β-catenin. (W) Co-injection of mRNAs for stabilized β-catenin and Smp-FL. (X) Overexpression of Smp-ΔNLS with stabilized β-catenin. Numbers in the lower or upper right panel corners represent number of embryos with the observed phenotype/the total number of embryos (also represented as a percentage). Scale bars: 50 μm in B-G; 100 μm in H-X. Numbers in the lower or upper right corners indicate the number of embryos with the depicted expression patterns/the total number of embryos.

Fig. S13). By contrast, co-injection of the mutant Smp-ΔNLS-GFP inhibited the activation of the Wnt reporter (Fig. 3X; supplementary material Fig. S13). Thus, retention of Smp in the cytoplasm inhibits β-catenin signaling, indicating that Smp nuclear localization is essential for nuclear localization and for the transcriptional activity of β-catenin.

The regulation of β-catenin-dependent Wnt signaling by Smp is conserved in mammals

The mammalian ortholog of Smp is family with sequence similarity 53-member B (Fam53b/Smp). The existence of Smp in several vertebrate species suggests that its function is conserved in all vertebrates. Therefore, we assessed whether Smp is present in the mouse intestinal crypts where Wnt signaling is active. Immunohistochemistry for Smp showed staining in the intestinal crypts (supplementary material Fig. S14A) overlapping with Olfm4-postive stem cells (supplementary material Fig. S14B) (van der Flier et al., 2009), where β-catenin-dependent signaling is important (van Es et al., 2012). Immunocytochemistry for human SMP in HEK293T cells showed foci in the nucleus (Fig. 4A,B), indicating that human SMP accumulates and functions in the nucleus. To determine whether human SMP is required for

Development (2014) 141, 3529-3539 doi:10.1242/dev.108415

β-catenin nuclear localization in human cells, we performed siRNA knockdown of Smp in HEK293T cells (supplementary material Fig. S15A-K) and examined the subcellular distribution of SMP and β-catenin. Compared with unstimulated controls (Fig. 4C,D), stimulation with Wnt3-conditioned medium increased nuclear localization of endogenous β-catenin (Fig. 4E), which was reduced after transfection with *smp* siRNA (Fig. 4F). Subcellular fractionation experiments for β-catenin localization showed significant reduction in nuclear β-catenin upon *smp* knockdown (Fig. 4G; supplementary material Fig. S15L). Likewise, compared with Wnt3-stimulated pBAR activation in control transfected cells, there was a significant reduction in β-catenin-mediated activation of pBAR reporter in Smp siRNA-transfected cells (Fig. 4H). These results support the conclusion from the *in vivo* experiments that Smp is required for β-catenin nuclear localization and transcriptional activity. To assess whether increasing human SMP mediates β-catenin transcriptional activity in a dose-dependent manner, as does zebrafish Smp, we overexpressed SMP with β-catenin in HEK293 cells enhanced the activity of the β-catenin-dependent pBAR reporter in a dose-dependent manner (Fig. 4I), as observed in zebrafish cells (supplementary material Fig. S11C).

The ability of SMP to regulate nuclear localization and transcriptional activity of β-catenin suggests that these two proteins interact. Co-expression and immunoprecipitation of the FLAG-tagged β-catenin with SMP-myc from HEK293T cell lysates showed an interaction between the two proteins (Fig. 4J), suggesting that proteins interact either directly or indirectly as part of a larger protein complex. Immunoprecipitation experiments with different deletion constructs showed that the first homology domain in Smp is required for their interaction (Fig. 4K; supplementary material Fig. S15M). To determine which region in β-catenin is required for its interaction with SMP, we performed co-immunoprecipitation experiments with several β-catenin deletion mutants lacking different stretches of the armadillo repeats or the N terminus preceding the repeats or the C terminus. We observed that the N terminus of β-catenin is required for interaction with SMP (Fig. 4L; supplementary material Fig. S15N,O).

Although co-transfection of full-length Smp enhanced β-catenin activation of the pBAR reporter, the SMP mutant lacking this β-catenin interaction domain (SMPΔHRI) showed a significant reduction in reporter activity after transfection with full-length β-catenin (supplementary material Fig. S15T) or with a stabilized mutant version of β-catenin (Fig. 4M) despite its localization to the nucleus (Fig. 4N). When we injected *smp*ΔHRI mRNA into early embryos, we did not observe any outstanding phenotypes, even after injection of mRNA (supplementary material Fig. S15R,S), unlike injection of *smp*-FL mRNA (supplementary material Fig. S15P,Q,S). We believe that lack of a phenotype from *smp*ΔHRI is due to the inability of the mutant protein to compete with the endogenous protein. We then assessed whether the interaction occurs in the cytoplasm or the nucleus and observed from co-immunoprecipitation experiments that a SMP-β-catenin complex existed primarily in the nucleus with a reduced interaction in the cytoplasm (Fig. 4O), indicating that they are part of a molecular complex that exists primarily in the nucleus.

The regulation of β-catenin activity involves its bidirectional nuclear translocation, and the regulation of its nuclear-cytoplasmic shuttling determines the amount of β-catenin available for transcription (Valenta et al., 2012). To assess whether SMP can alter β-catenin subcellular distribution, we performed fluorescence recovery after photobleaching (FRAP) experiments by bleaching mCherry-tagged β-catenin expressed in HEK293 cells in the presence of GFP or SMP-GFP. The measured decrease in the nuclear fraction of β-catenin in GFP-expressing cells after photobleaching mCherry in the cytoplasm indicates how much β-catenin has mobilized out of the nucleus (Fig. 4P, green nuclear curve). This reduction in nuclear β-catenin in cells transfected with control GFP is associated with an increase in β-catenin in the photobleached cytoplasm (Fig. 4P, green cyto curve). By comparison, photobleaching the cytoplasm of Smp-GFP-expressing cells showed less of a reduction in nuclear β-catenin (Fig. 4P, red nuclear curve) that was accompanied by a reduced cytoplasmic recovery (Fig. 4P, red cyto curve). Conversely, when we photobleach the nucleus, we do not observe statistically significant differences in the recovery of β-catenin into the nucleus between GFP-control transfected and SMP-GFP transfected cells (supplementary material Fig. S15U, black bracket), indicating that SMP is not facilitating β-catenin nuclear import.

DISCUSSION

We identify Smp as a novel regulator of the β-catenin-dependent Wnt signal transduction pathway, because it is required for this pathway, and because it is sufficient to enhance β-catenin nuclear localization. *smp* expression and its subcellular distribution do not appear to be regulated by Wnt signaling, and it is not sufficient to promote β-catenin transcriptional activity without Wnt stimulation, indicating that Smp acts on the pathway after Wnt-mediated accumulation of β-catenin.

Previous work showed that Smp is required for proliferation of the early embryonic cells (Thermes et al., 2006). Although Smp shares stretches of identical amino acid sequence with Fam53A (31% identical) and Fam53C (33% identical), these proteins have not been characterized, so it is unclear what the biological functions of these proteins are and whether they have overlapping functions with Smp or with each other. Our observations that the first homology domain in Smp is required for its interaction with β-catenin and that this domain has conserved stretches of identical amino acid sequences in Fam53A and Fam53C, suggests that they too may regulate the nuclear localization of β-catenin.

Like Smp, Wnt signaling is also required for cell proliferation (Niehrs and Acebron, 2012), but our evidence that inhibiting cell proliferation does not affect β-catenin-dependent transcription (supplementary material Fig. S6) indicates that the regulation of cell proliferation by Smp is either independent of its role in β-catenin nuclear localization or is mediated by β-catenin-dependent signaling. Yeast two-hybrid screens and immunoprecipitation experiments indicate that Smp has other partners in addition to β-catenin: the ski-interacting protein (Skiip) and 14-3-3 (Thermes et al., 2006). The oncogene Ski is involved in cell proliferation, cell differentiation, transformation and tumor progression (Bonnon and Atanasoski, 2012), and one function of this protein is to regulate Tgf signaling by adjusting the downstream activity of Smad (Bonnon and Atanasoski, 2012). In addition to interacting with Ski, Skiip interacts with Epstein Barr virus, NotchIC, Myc and menin of the histone methyltransferase Mll1 (Zhou et al., 2000a,b; Bres et al., 2009). The interaction between Smp and Skiip suggests that Smp may be involved in the activities of these other proteins, but this remains to be determined. Smp has several 14-3-3 binding sites (Thermes et al., 2006), and we confirmed that 14-3-3 isoforms do immunoprecipitate with Smp, suggesting that they may be involved in regulating the interaction of Smp with β-catenin. Co-immunoprecipitation experiments that we performed showed that β-catenin can be pulled down with Smp together with 14-3-3 or independently of it (data not shown), indicating that 14-3-3 presence or absence does not have a role in regulating β-catenin interaction with Smp.

Development (2014) 141, 3529-3539 doi:10.1242/dev.108415

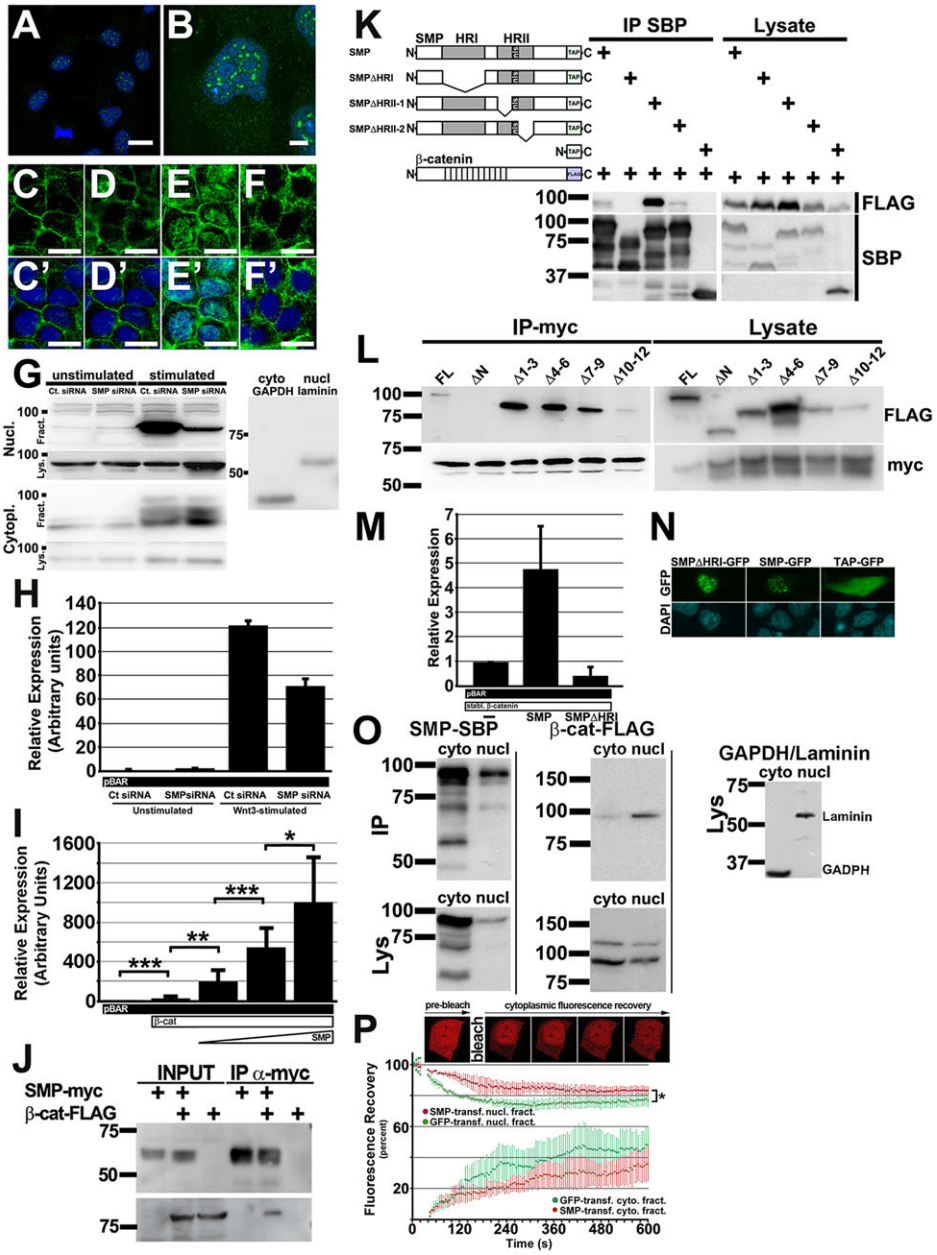

Fig. 4. Mammalian SMP (FAM53B) regulates β-catenin similarly to zebrafish Smp and interacts with β-catenin to retain it in the nucleus.
(A) Immunocytochemistry (ICC) for the human SMP (green) in the Hoechst-stained nuclei (blue) of HEK293T cells. (B) Higher magnification shows the protein localizes as foci in Hoechst-stained nuclei. (C-F) β-Catenin ICC (green) of control siRNA-transfected unstimulated HEK293T cells (C), SMP siRNA-transfected HEK293T cells (D). control siRNA-transfected HEK293T cells stimulated with Wnt3-conditioned medium (E) and SMP siRNA-transfected HEK293T cells stimulated with Wnt3-conditioned medium (F). (C′-F′) β-Catenin ICC merged with DAPI (blue). (G) Representative subcellular fractionation blots showing the protein levels of nuclear (Nucl.) and cytoplasmic (Cytopl.) β-Catenin in unstimulated and Wnt3-stimulated HEK293T cells transfected either with control (Ctr) siRNA or Smp siRNA. Fract. denotes nuclear or cytoplasmic fractionation blots. Lys. denotes blots for loading control of total lysates for each fraction. Laminin and GAPDH show clear separation of the fractions. The numbers indicate protein ladder positions in kDa. (H) Fold activation of pBAR luciferase reporter from assays of control and Smp siRNA knockdown HEK293T cells without and with Wnt3-condition medium stimulation (Wnt). $P<0.01$ between Ct and SMP siRNA Wnt3-stimulated groups. Data are the average±s.d. (I) Dose-dependent activation of β-catenin-responsive promoter by human SMP. $*P<0.05$, $**P<0.001$, $***P<0.008$. Data are the average±s.d. (J) Immunoprecipitation blot using anti-Myc antibody to pull down Myc-tagged human SMP shows co-immunoprecipitation of Flag-tagged human β-catenin as detected by anti-Flag antibody. (K) Immunoprecipitation experiment using different TAP-Tagged (TAP) SMP deletion mutants to determine which conserved domain interacts with FLAG-tagged β-catenin. (L) Immunoprecipitation experiment of SMP-myc for different FLAG-tagged β-catenin deletion mutants lacking either the N terminus or different sets of armadillo repeats. The lysate gels show the level of expression of each construct. (M) Luciferase assay of HEK293T cells transfected with: pBAR and stabilized β-catenin; pBAR, stabilized β-catenin and full-length SMP; or pBAR, stabilized β-catenin and SMP lacking the first homology domain (SMP-ΔHRI). $P<0.01$ between all groups. Data are the average±s.d. (N) Transfection of HEK293T cells with TAP-tagged GFP or SMP-GFP or SMP-ΔHRI-GFP shows nuclear localization of both SMP expression constructs. (O) Blot of subcellular fractionation (nuclear versus cytoplasmic) experiment for transfected TAP-tagged Smp and FLAG-tagged β-catenin. Immunoprecipitation blots (IP) are above. Lysate blots (Lys) are below. Lysate blot probed with GAPDH and laminin shows clear separation of each fraction. (P) β-Catenin-mCherry fluorescence before bleaching and at increasing times after photobleaching the cytoplasm of HEK293T cells co-transfected either with GFP or SMP-GFP. The graph shows the decrease in nuclear β-catenin-mCherry and its cytoplasmic recovery. $*P<0.05$. Scale bars: 20 µm in A,B; 5 µm in C-F′. Data represent at least three or more independent experiments.

Development (2014) 141, 3529-3539 doi:10.1242/dev.108415

Several phenomena are necessary for the nuclear localization of β-catenin: stabilization of β-catenin in the cytoplasm, and its transport to the nucleus and its subsequent retention there (MacDonald et al., 2009). Previous work has shown that the nuclear export of β-catenin is promoted by the Ran-binding protein 3 (Ranbp3) (Hendriksen et al., 2005), which has been shown to interact with Crm1 and Ran-GTP, and consequently to promote nuclear export of proteins with lysine-rich nuclear export sequences (Nemergut et al., 2002). However, promotion of β-catenin nuclear export by Ranbp3 appears to be independent of Crm1 (Hendriksen et al., 2005). It has also been shown that β-catenin can enter the nucleus independent of Ran GTPase and importin-mediated mechanisms (Fagotto et al., 1998; Yokoya et al., 1999; Eleftheriou et al., 2001; Wieschens and Fagotto, 2001), and it does so using intrinsic nuclear import and export information within specific armadillo repeats (Asally and Yoneda, 2005; Sharma et al., 2012). By contrast, the familial adenomatous polyposis and colon cancer (*Apc*) gene, the nuclear import and export of which involves importin and exportin-mediated transport, has been shown to regulate both nuclear and cytoplasmic shuttling of β-catenin (Henderson, 2000). Although the requirement for Smp for β-catenin nuclear localization could involve either a shuttling or a retention mechanism, the difference in the steady state plateau values after photobleaching the cytoplasm indicate that Smp affects the mobility of β-catenin from the nucleus, and the lack of a significant difference after bleaching the nucleus argues that Smp has less effect on the movement of β-catenin from the cytoplasm into the nucleus. We do not know whether Smp is involved in transporting β-catenin through the nuclear pore or whether it promotes nuclear β-catenin by sequestration in a chromatin or transcription factor complex, as happens with Foxm1 (Zhang et al., 2011).

Other proteins have been shown to regulate β-catenin activity by perturbing its interaction with its transcription partner Lef1/Tcf (e.g. Drapper and Chibby), by shuttling it out of the nucleus (e.g. Drapper, Chibby, Apc) and by promoting its degradation (e.g. Apc) (Ahmed et al., 1998; Gao et al., 2008; Li et al., 2008, 2010). These proteins negatively regulate β-catenin nuclear distribution, while Smp positively regulates it, so it is unlikely that Smp promotes β-catenin nuclear localization through the interaction with these proteins. Both Smp and β-catenin can interact with 14-3-3 proteins (Tian et al., 2004; Thermes et al., 2006); however, we have not observed simultaneous interaction of the three proteins. The interaction between Smp and β-catenin requires the N-terminal sequences of β-catenin, but most known regulators of β-catenin function interact within specific armadillo repeat sequences within β-catenin, so it remains unclear whether Smp regulates nuclear localization of β-catenin by impacting the function of any of the known β-catenin regulators. Future work on defining the co-factors that function together with Smp will provide insight into how Smp promotes β-catenin nuclear localization.

Immunocytochemistry experiments show that endogenous Smp can localize broadly or at foci in the nucleus, and that its nuclear localization overlaps with β-catenin. It is not yet clear whether the location of the foci in the nucleus is arbitrary or targeted to specific sites. Although the protein has conserved domains, there are no similarities to protein domains whose function is known, so the activities of these domains still need to be characterized. Other than the requirement for the first domain to maintain β-catenin in the nucleus, it is not yet clear whether Smp serves simply to keep β-catenin in the nucleus or to promote the localization of β-catenin to specific sites.

The ability of Smp to regulate β-catenin-dependent signaling in the embryo and its presence in the crypts of the intestine support the conclusion that Smp is involved in regulation of β-catenin-dependent Wnt signaling of stem and progenitor cells. Our observation that *smp* mRNA and protein do not change their expression levels or subcellular distribution after modulating Wnt signaling (Fig. 2L-N,Z,AA; supplementary material Fig. S12) indicates that Smp expression and nuclear localization is independent of β-catenin-dependent Wnt signaling. We postulate that Smp is a regulatory node either as an adapter or as a protein with an additional function through which other signal transduction pathway regulate/influence the subcellular distribution of β-catenin. Whether Smp is required in all Wnt signaling contexts or whether there are other factors that perform a similar activity needs to be determined. The broad distribution of the *smp* transcript and the protein (supplementary material Fig. S1) in the progenitor cells of the early embryo and its reactivation in the adult during zebrafish regeneration (Kizil et al., 2009) rather than their strict localization to regions of active β-catenin-dependent Wnt signaling argues that Smp has other functions in addition to regulating β-catenin subcellular distribution. What these functions are still needs to be determined.

In addition to embryonic development, Smp is required for tissue regeneration (Kizil et al., 2009). Based on our findings in the embryo, it is likely that the requirement for Smp during regeneration includes its regulation of Wnt signaling. To date there are no known mutations in Smp associated with disease that aid in understanding the physiological importance of the conserved domains, but there are correlations between increased Smp expression and multiple melanoma (Clevers, 2006; Agnelli et al., 2011). Future experiments will determine what molecular signals are involved in regulating Smp activity and how this regulation modifies the Wnt signal transduction cascade in embryonic and regenerative contexts.

MATERIALS AND METHODS

Fish maintenance and husbandry

Fish were maintained at 28°C (Brand et al., 2002). All procedures were carried out in accordance with the live animal handling and research regulations under protocols approved by the animal welfare committees of the Technische Universität Dresden and the Landesdirektion Sachsen. For heat-shock experiments, embryos were placed at 37°C for 1 h at 60% epiboly.

Morpholino and mRNA injections

Previously characterized morpholino oligonucleotides for *smp* (4 ng) and *p53* (3 ng) (Kizil et al., 2009; Robu et al., 2007) were injected into one-cell stage embryos with glass capillaries (World Precision Instruments, TWF10). Capped *smp* mRNA (20 pg), 20 pg *smp*ΔNLS (Kizil et al., 2009) and/or 2 pg of *wnt8* mRNA (Weidinger et al., 2005), or 2 pg of stabilized β-catenin mRNA were injected similarly.

In situ hybridization

In situ hybridization for fish was performed as described previously (Jowett and Lettice, 1994) using VSi In Situ Robot (Intavis). Probes were transcribed from linearized templates using DIG-labeled NTPs (Roche). Bright-field or DIC images were taken using AxioCam compound microscope (Zeiss). Intestines from adult mice were dissected and flushed gently with PBS prior to fixation in 10% formalin overnight. Samples were then dehydrated and embedded in paraffin. *In situ* hybridization was performed on 5 µm sections as described previously (Gregorieff and Clevers, 2005). The probe against Olfm4 was generated by linearizing pBluescript Olfm4 with *Not*I and *in vitro* transcription with T7 (Roche).

Cell-tracking experiments

Embryos were injected with either *Smp* antisense or *Smp* mismatch morpholino at the one-cell stage. At 50% epiboly, 5 pg tracker dye (CellTrackerTM Red CMTPX, Invitrogen) was injected into the region that

Development (2014) 141, 3529-3539 doi:10.1242/dev.108415

forms the somitic or head mesoderm, according to the fate map of zebrafish embryo (Kimmel et al., 1990). Labeled cells were detected 10 minutes after injection with red fluorescence. The level of convergent extension was checked at tailbud stage by alignment of labeled cells at the midline and the anterior region.

Calculation of mitotic indices

Mitotic indices were calculated by counting the total number of H3P-positive cells per mm^2. Statistical analyses were performed using Excel software and *t*-test.

Apoptosis assay

Apoptotic cells were detected by TUNEL (Fluorescence In Situ Cell Death Detection Kit, Roche) and AnnexinV-Cy3 (BioVision) stainings, as instructed by the manufacturer. Images were obtained using epifluorescence microscope (Zeiss Apotome).

Hydroxyurea and aphidicolin treatment of embryos

Hydroxyurea (20 mM, Sigma) and aphidicolin (150 µM, Merck) were dissolved in E3 fish water (Brand et al., 2002). Embryos were treated starting at 4 hours post-fertilization in Petri dishes until desired developmental stage.

Immunohistochemistry

Antibody staining was performed using anti-Tbx16 (mouse, 1:100, ZIRC), anti-Dlx3b (mouse, 1:50, ZIRC), anti-Myf5 (rabbit polyclonal, recognizes MyoD, 1:50, Santa Cruz, sc-302), anti-H3p [rabbit polyclonal, 1:100, Upstate (Merck Millipore), 06-570], zebrafish anti-Smp [rabbit polyclonal; 1:600) (for generation of antibody, see the methods in the supplementary material), human anti-SMP (rabbit polyclonal, 1:400, Sigma, SAB1303084) and anti-β-catenin (rabbit polyclonal, 1:200, NEB, #9562) (Kizil et al., 2009). Goat anti-mouse Cy3 (1:500, Dianova, 115-165-146), goat anti-rabbit Alexa-488 (1:200, Molecular Probes, Invitrogen, 111-545-144) secondary antibodies were used. Images were taken with fluorescence ApoTome microscope (Zeiss). For mouse intestines, 7 µm sections were deparaffinized and rehydrated. Antigen retrieval was performed by boiling samples for 20 min in EDTA buffer [1 mM EDTA, 0.05% Tween 20 (pH 8)] and then cooled to room temperature. Endogenous peroxidase was blocked by incubation 15 min in 0.9% H_2O_2. Sections were blocked with 10% goat serum (Vector Laboratories) in 1× PBS for 30 min. The SMP antibody (Sigma) was diluted in 2% BSA in PBS and the HRP anti-rabbit secondary antibody (GE Healthcare) in 10% NGS. Incubation of primary antibody was performed overnight at 4°C and secondary antibody for 1 h at room temperature. The staining was developed using Sigma*FAST* 3,3′-diaminobenzidine tablets following the manufacturer's instructions. Sections were mounted in 70% glycerol for imaging.

Transgenic lines

Transgenic Wnt reporter line Tg(7xTCF-XLa.Siam:nlsmCherry)^{ia5} (Kwan et al., 2007; Moro et al., 2012). Other transgenic lines were Tg(Top:dGFP) (Dorsky et al., 2002), Tg(*hsp70*:*dkk1*-GFP) and Tg(*hsp70*:*wnt8a*-GFP) (Stoick-Cooper et al., 2007), and Tg(*hsp70*:GFP) (Halloran et al., 2000).

Luciferase assays

smp mRNA was generated from the clone IRATp970D074D (ImaGenes). *smp* was subcloned into the pcDNA3 myc-His expression vector (Invitrogen) via *Bam*HI sites. HEK293 cells grown at 37°C in 10% FCS serum (Biochrom AG) in DMEM (Gibco) were transfected with *smp* expression plasmid and with other plasmids containing *wnt8*, *dsh*, β-catenin, and the Renilla and Luciferase reporters (Weidinger et al., 2005) using FuGene 6 (Roche). Firefly and Renilla activities were measured from cell lysates using the Dual-Luciferase Reporter Assay System (Promega) 24 h after transfection.

Immunoprecipitation experiments

HEK293T cells were transfected with pCS2-FLAG-tagged β-catenin, pcDNA6-SMP-Myc or pcDNA6-SMP-SBP (Streptavidin Binding Protein) as designated using the Fugene 6 reagent (Roche) according to manufacturer's instructions with a DNA:Fugene ratio of 1:2. Forty-eight hours after transfection, cells were trypsinized and washed subsequently with PBS and cell buffer [10% glycerol; 75 mM Hepes, KOH 7.4, 150 mM KCl, 2 mM $MgCl_2$, 2 mM EDTA]. Cells were lysed in cell buffer supplemented with 0.1% NP40 and 1× protease and phosphatase Inhibitor cocktails (Roche). Co-immunoprecipitations were performed with the MultiMACS Epitope tag isolation kit (Miltenji Biotec). Cell lysates were centrifuged for 10 min at 16,000 ***g*** at 4°C. An aliquot (50 µl) of the supernatant was boiled with 2× SDS-SB as input. The residual 200 µl were transferred into a new tube and incubated with 50 µl µMACS anti-c-myc MicroBeads (Miltenji Biotec) or 50 µl anti-streptavidin beads (Pierce) for 30 min on ice. Labeled proteins were loaded onto with lysis buffer preconditioned µ Columns (Miltenji Biotec) or centrifuged for 10 min at 16,000 ***g***, and washed with 1 ml lysis buffer and subsequently 100 µl wash buffer 2 (Miltenji Biotec). Elution of proteins was achieved with preheated Elution buffer (Miltenji Biotec).

Nuclear fractionation and western blotting

Nuclei from tailbud embryos were isolated using a glass-glass homogenizer and differential centrifugation ((German and Howe, 2009). Nuclei were lysed [50 mM Tris-HCl (pH 8.0), 10 mM EDTA, 2% SDS, 1× proteinase inhibitor cocktail (Roche)] and the lysate was separated by centrifugation (16,000 ***g***, 4°C, 10 min). Samples were loaded to 10% SDS-PAGE gels. Proteins were transferred to a 0.45 µm sieved PVDF membrane (Roth) by electroblotting. Rabbit anti-β-catenin (1:2000, NEB), rabbit anti-FLAG (1:500, Sigma), mouse anti-myc (1:400, Upstate), anti-streptavidin-binding protein (SBP) (1:20,000, Millipore), ECL Plex goat anti-mouse HRP (1:4000, GE Life Sciences) and donkey anti-rabbit HRP (1:4000, GE Life Sciences) were used. Membrane was washed with hybridization buffer [25 mM Tris, 192 mM glycine (pH 8.3)] for 1 h and signal was detected using chemiluminescence kit (ECL Western Blotting Detection Kit, GE Life Sciences). As loading controls, γ-tubulin (1:2000, NEB) and GFP (H2A-GFP transgenic line, 1:2000, Millipore) were used. Band intensities are calculated using Fiji software (http://pacific.mpi-cbg.de/wiki/index.php/Main_Page).

siRNA knockdown experiments

HEK293T cells were incubated for 24 h in reduced serum conditions (1% FBS) and then transfected with Stealth siRNA (Invitrogen) using RNAi MAX lipofectamine (Invitrogen). After 48 h, cells were transfected with plasmid reporter and expression constructs and incubated for 24 h before treating with Wnt3-conditioned medium. Cells were lysed after 8 h and Firefly and Renilla activities were measured from cell lysates using the Dual-Luciferase Reporter Assay System (Promega).

Photobleaching experiments

FRAP analysis was performed with HEK293T cells 24 h post transfection (300 ng/well pCS2+ β-catenin-mCherry and 30 ng/well pCS2+ FAM53B-GFP or equimolar amounts of peGFP) in a Lab-TekII eight-well chamber (ThermoScientific) at 37°C in DMEM (Gibco). Nuclei were counterstained with 1.7 ng/ml Hoechst 33342 before imaging. Photobleaching was performed on a confocal microscope Zeiss LSM780 with an attached ConfoCor3-detection module using Zen 2010 software. EGFP was excited by the 488 nm (Argon laser), Hoechst 33342 by a 405 nm laser diode and β-catenin-mCherry by a 561 DPSS laser. Fluorescence imaging was sequential using three channels: EGFP, 489-559 nm on the GaAsP-detector; Hoechst 33342, a BP 420-475 band using a APD detector of the ConfoCor3 module; mCherry, a LP580 band with a APD detector of the ConfoCor3 module. Imaging used low laser power for all channels (EGFP <1%, 0.263 µW; Hoechst 33342, 0.2%, 14 µW; mCherry, <0.6%, 0.447 µW). Bleaching was with high laser power (100%, 197 µW) and enhanced bleaching using the 488 nm and 514 nm lines of the Argon laser (100%, 129 µW and 69.9 µW, respectively). The cell compartments were bleached with 16 separate point bleaches at a low scanning speed for a period of 15.49 s. Bleaching effects were minimized by using low laser power and fast imaging speed (1.94 s). The fluorescence in the cytoplasm was bleached by 60-70% of the initial images and was taken as a reference. After the bleaching, images were taken every 5 s for 14 min. Average intensities in

Development (2014) 141, 3529-3539 doi:10.1242/dev.108415

regions of interest were measured with ImageJ. The ratio of the average fluorescence in the bleached area (nucleus or cytoplasm) over the unbleached compartment (cytoplasm or nucleus) was plotted over time. The ratio in the pre-bleach image was set to 100% and the first post-bleach image was set to 0%. The recovery curves are averages of four experiments with 15/16 cells (FAM53B/GFP) and three experiments with 11/12 cells (GFP/FAM53B) for cytoplasmic bleaches and nuclear bleaches, respectively.

Acknowledgements

We thank R. Paul for the generation of the zebrafish antibody at the CRTD Protein Facility. We also thank D. Drechsel for advice on protein work, C. Nüsslein-Volhard for her support, C. Bökel and K. Neugebauer for their helpful discussions and advice, and M. Michel for help with statistical analysis. The human β-catenin-FLAG was a gift from the Schambony Lab.

Competing interests

The authors declare no competing financial interests.

Author contributions

All authors contributed to the design of the research. Expression analyses were performed by C.K., B.K. and J.-J.Y. The morpholino knockdown experiments were performed by C.K. and J.-J.Y. The subcellular distribution studies were performed by C.K., C.L.A. and J.-J.Y. The transcriptional assays were performed by B.K., C.L.A. and G.Ö. The *in vivo* overexpression studies were performed by B.K. and C.L.A. The immunohistochemistry experiments were performed by B.K. and J.-J.Y. The FRAP experiments were performed by B.K. The siRNA knockdown experiments were performed by J.-J.Y., C.L.A. and C.K. F.A. and E.M. produced the transgenic Wnt reporter line. G.W. supervised transcriptional assays, suggested experiments and contributed to the writing of the manuscript.

Funding

This work was supported by the Deutsche Forschungsgemeinschaft (DFG) to G.Ö., G.W., M.B. and C.L.A. [SFB655 and AN797/1-1] as well as by the Max-Planck Gesellschaft (C.K. and C.L.A.). F.A. and E.M. are supported by CARIPARO 'Cancer biosensors', AIRC IG10274 and the EU ZF-HEALTH Large-scale Integrated Project in the 7th Framework Programme [242048-2].

Supplementary material

Supplementary material available online at
http://dev.biologists.org/lookup/suppl/doi:10.1242/dev.108415/-/DC1

References

Agathon, A., Thisse, C. and Thisse, B. (2003). The molecular nature of the zebrafish tail organizer. *Nature* **424**, 448-452.

Agnelli, L., Forcato, M., Ferrari, F., Tuana, G., Todoerti, K., Walker, B. A., Morgan, G. J., Lombardi, L., Bicciato, S. and Neri, A. (2011). The reconstruction of transcriptional networks reveals critical genes with implications for clinical outcome of multiple myeloma. *Clin. Cancer Res.* **17**, 7402-7412.

Ahmed, Y., Hayashi, S., Levine, A. and Wieschaus, E. (1998). Regulation of armadillo by a Drosophila APC inhibits neuronal apoptosis during retinal development. *Cell* **93**, 1171-1182.

Angers, S. and Moon, R. T. (2009). Proximal events in Wnt signal transduction. *Nat Rev Mol Cell Biol* **10**(7), 468-77.

Aoki, M., Hecht, A., Kruse, U., Kemler, R. and Vogt, P. K. (1999). Nuclear endpoint of Wnt signaling: neoplastic transformation induced by transactivating lymphoid-enhancing factor 1. *Proc. Natl. Acad. Sci. USA* **96**, 139-144.

Asally, M. and Yoneda, Y. (2005). beta-Catenin can act as a nuclear import receptor for its partner transcription factor, lymphocyte enhancer factor-1 (lef-1). *Exp. Cell Res.* **308**, 357-363.

Bonnon, C. and Atanasoski, S. (2012). c-Ski in health and disease. *Cell Tissue Res.* **347**, 51-64.

Brand, M., Granato, M. and Nüsslein-Volhard, C. (2002). Keeping and raising zebrafish. In *Zebrafish: A Practical Approach* (ed. R. Dahm and C. Nüsslein-Volhard), pp. 7-37. Oxford: Oxford University Press.

Brès, V., Yoshida, T., Pickle, L. and Jones, K. A. (2009). SKIP interacts with c-Myc and Menin to promote HIV-1 Tat transactivation. *Mol. Cell* **36**, 75-87.

Cavodeassi, Florancia (2013). Integration of anterior neural plate patterning and morphogenesis by the wnt signaling pathway. *Developmental Neurobiology* **74**, 759-771.

Chapman, D. L. and Papaioannou, V. E. (1998). Three neural tubes in mouse embryos with mutations in the T-box gene Tbx6. *Nature* **391**, 695-697.

Christian, J. L. and Moon, R. T. (1993). Interactions between Xwnt-8 and Spemann organizer signaling pathways generate dorsoventral pattern in the embryonic mesoderm of *Xenopus*. *Genes Dev* **7**, 13-28.

Clevers, H. (2006). Wnt/beta-catenin signaling in development and disease. *Cell* **127**, 469-480.

Dorsky, R. I., Sheldahl, L. C. and Moon, R. T. (2002). A transgenic Lef1/β-catenin-dependent reporter is expressed in spatially restricted domains throughout Zebrafish development. *Dev. Biol.* **241**, 229-237.

Du, S. J., Purcell, S. M., Christian, J. L., McGrew, L. L. and Moon, R. T. (1995). Identification of Distinct Classes and Functional Domains of Wnts through Expression of Wild-type and Chimeric Proteins in *Xenopus* Embryos. *Mol. Cell. Biol.* **15**, 2625-2634.

Eleftheriou, A., Yoshida, M. and Henderson, B. R. (2001). Nuclear export of human β-catenin can occur independent of CRM1 and the adenomatous polyposis coli tumor suppressor. *J. Biol. Chem.* **276**, 25883-25888.

Erter, C. E., Wilm, T. P., Basler, N., Wright, C. V. E. and Solnica-Krezel, L. (2001). Wnt8 is required in lateral mesendodermal precursors for neural posteriorization in vivo. *Development* **128**, 3571-3583.

Fagotto, F., Glück, U. and Gumbiner, B. M. (1998). Nuclear localization signal-independent and importin/karyopherin-independent nuclear import of β-catenin. *Curr. Biol.* **8**, 181-190.

Gao, X., Wen, J., Zhang, L., Li, X., Ning, Y., Meng, A. and Chen, Y.-G. (2008). Dapper1 is a nucleocytoplasmic shuttling protein that negatively modulates wnt signaling in the nucleus. *J. Biol. Chem.* **283**, 35679-35688.

German, C. L. and Howe, C. L. (2009). Preparation of biologically active subcellular fractions using the Balch homogenizer. *Anal. Biochem.* **394**, 117-124.

Glinka, A., Wu, W., Delius, H., Monaghan, A. P., Blumentstock, C. and Niehrs, C. (1998). Dickkopf-1 is a member of a new family of secreted proteins and functions in head induction. *Nature* **391**, 357-362.

Gregorieff, A. and Clevers, H. (2005). Wnt signaling in the intestinal epithelium: from endoderm to cancer. *Genes Dev.* **19**, 877-890.

Grigoryan, T., Wend, P., Klaus, A. and Birchmeier, W. (2008). Deciphering the function of canonical Wnt signals in development and disease: conditional loss- and gain-of-function mutations of β-catenin in mice. *Genes Dev.* **22**, 2308-2341.

Halloran, M. C., Sato-Maeda, M., Warren, J. T., Su, F., Lele, Z., JKrone, P. H., Kuwada, J. Y. and Shoji, W. (2000). Laser-induced expression in specific cells of transgenic zebrafish. *Development* **127**, 1953-1960.

Heisenberg, C.-P., Tada, M., Rauch, G.-J., Saúde, L., Concha, M. L., Geisler, R., Stemple, D. L., Smith, J. C. and Wilson, S. W. (2000). Silberblick/Wnt11 mediates convergent extension movements during zebrafish gastrulation. *Nature* **405**, 76-81.

Henderson, B. R. (2000). Nuclear-cytoplasmic shuttling of APC regulates β-catenin subcellular localization and turnover. *Nat. Cell Biol.* **2**, 653-660.

Hendriksen, J., Fagotto, F., van der Velde, H., van Schie, M., Noordermeer, J. and Fornerod, M. (2005). RanBP3 enhances nuclear export of active β-catenin independently of CRM1. *J. Cell Biol.* **171**, 785-797.

Jowett, T. and Lettice, L. (1994). Whole-mount in situ hybridizations on zebrafish embryos using a mixture of digoxigenin- and fluorescein-labelled probes. *Trends Genet.* **10**, 73-74.

Kelly, G. M., Erezyilmaz, D. F. and Moon, R. T. (1995). Induction of a secondary embryonic axis in zebrafish occurs following the overexpression of *b-catenin*. *Mech Dev* **53**, 261-273.

Kiecker, C. and Niehrs, C. (2001). A morphogen gradient of wnt/b-catenin signaling regulates anteroposterior neural patterning in *Xenopus*. *Development* **128**, 4189-4201.

Kilian, B., Mansukoski, H., Barbosa, F. C., Ulrich, F., Tada, M. and Heisenberg, C.-P. (2003). The role of Ppt/Wnt5 in regulating cell shape and movement during zebrafish gastrulation. *Mech. Dev.* **120**, 467-476.

Kizil, C., Otto, G. W., Geisler, R., Nüsslein-Volhard, C. and Antos, C. L. (2009). Simplet controls cell proliferation and gene transcription during zebrafish caudal fin regeneration. *Dev. Biol.* **325**, 329-340.

Kwan, K. M., Fujimoto, E., Grabher, C., Mangum, B. D., Hardy, M. E., Campbell, D. S., Parant, J. M., Yost, H. J., Kanki, J. P. and Chien, C.-B. (2007). The Tol2kit: a multisite gateway-based construction kit for Tol2 transposon transgenesis constructs. *Dev. Dyn.* **236**, 3088-3099.

Lekven, A. C., Thorpe, C. J., Waxman, J. S. and Moon, R. T. (2001). Zebrafish *wnt8* encodes two Wnt8 proteins on a bicistronic transcript and is required for mesoderm and neuroectoderm patterning. *Dev. Cell* **1**, 103-114.

Leyns, L., Bouwmeester, T., Kim, S.-H., Piccolo, S. and De Robertis, E. M. (1997). Frzb-1 is a secreted antagonist of Wnt signaling expressed in the spemann organizer. *Cell* **88**, 747-756.

Li, F.-Q., Mofunanya, A., Harris, K. and Takemaru, K.-I. (2008). Chibby cooperates with 14-3-3 to regulate β-catenin subcellular distribution and signaling activity. *J. Cell Biol.* **181**, 1141-1154.

Li, F.-Q., Mofunanya, A., Fischer, V., Hall, J. and Takemaru, K.-I. (2010). Nuclear-cytoplasmic shuttling of chibby controls β-catenin signaling. *Mol. Biol. Cell* **21**, 311-322.

MacDonald, B. T., Tamai, K. and He, X. (2009). Wnt/β-catenin signaling: components, mechanisms, and diseases. *Dev. Cell* **17**, 9-26.

Moro, E., Ozhan-Kizil, G., Mongera, A., Beis, D., Wierzbicki, C., Young, R. M., Bournele, D., Domenichini, A., Valdivia, L. E. and Lum, L. et al. (2012). *In vivo* Wnt signaling tracing through a transgenic biosensor fish reveals novel activity domains. *Dev. Biol.* **366**, 327-340.

Nemergut, M. E., Lindsay, M. E., Brownawell, A. M. and Macara, I. G. (2002). Ran-binding protein 3 links crm1 to the ran guanine nucleotide exchange factor. *J. Biol. Chem.* **277**, 17385-17388.
Niehrs, C. and Acebron, S. P. (2012). Mitotic and mitogenic Wnt signalling. *EMBO J.* **31**, 2705-2713.
Petersen, C. P. and Reddien, P. W. (2009). Wnt signaling and the polarity of the primary body axis. *Cell* **139**, 1056-1068.
Pilon, N., Oh, K., Sylvestre, J.-R., Bouchard, N., Savory, J. and Lohnes, D. (2006). Cdx4 is a direct target of the canonical Wnt pathway. *Dev. Biol.* **289**, 55-63.
Popperl, H., Schmidt, C., Wilson, V., Hume, C.R., Dodd, J., Krumlauf, R. and Beddington, R.S. (1997). Misexpression of Cwnt8C in the mouse induces an ectopic embryonic axis and causes a truncation of the anterior neuroectoderm. *Development* **124**, 2997-3005.
Rhinn, M., Lun, K., Luz, M., Werner, M. and Brand, M. (2005). Positioning of the midbrain-hindbrain boundary organizer through global posteriorization of the neuroectoderm mediated by Wnt8 signaling. *Development* **132**, 1261-1272.
Rhinn, M., Picker, A. and Brand, M. (2006). Global and local mechanisms of forebrain and midbrain patterning. *Curr. Opin. Neurobiol.* **16**, 5-12.
Rhinn, M., Lun, K., Arendt, R., Werner, M. and Brand, M. (2009). Zebrafish gbx1 refines the midbrain-hindbrain boundary border and mediates the Wnt8 posteriorization signal. *Neural Dev.* **2**, 4-12.
Robu, M. E., Larson, J. D., Nasevicius, A., Beiraghi, S., Brenner, C., Farber, S. A. and Ekker, S. C. (2007). p53 activation by knockdown technologies. *PLoS Genet.* **3**, e78.
Roszko, I., Sawada, A. and Solnica-Krezel, L. (2009). Regulation of convergence and extension movements during vertebrate gastrulation by the Wnt/PCP pathway. *Semin. Cell Dev. Biol.* **20**, 986-997.
Schier, A. F. (2001). Axis formation and patterning in zebrafish. *Curr. Opin. Genet. Dev.* **11**, 393-404.
Schier, A. F. and Talbot, W. S. (2005). Molecular genetics of axis formation in zebrafish. *Annu. Rev. Genet.* **39**, 561-613.
Sharma, M., Jamieson, C., Johnson, M., Molly, M. P. and Henderson, B. R. (2012). Specific armadillo repeat sequences facilitate β-catenin nuclear transport in live cells via direct binding to nucleoporins NUP62, NUP153 and RanBP2/NUP358. *J. Biol. Chem.* **287**, 819-831.
Shimizu, T., Bae, Y.-K., Muraoka, O. and Hibi, M. (2005). Interaction of Wnt and caudal-related genes in zebrafish posterior body formation. *Dev. Biol.* **279**, 125-141.
Stoick-Cooper, C. L., Weidinger, G., Riehle, K. J., Hubbert, C., Major, M. B., Fausto, N. and Moon, R. T. (2007). Distinct Wnt signaling pathways have opposing roles in appendage regeneration. *Development* **134**, 479-489.
Tada, M. and Smith, J. C. (2000). Xwnt11 is a target of Xenopus Brachyury: regulation of gastrulation movements via dishevelled, but not through the canonical Wnt pathway. *Development* **127**, 2227-2238.
Takada, S., Stark, K. L., Shea, M. J., Vassileva, G., McMahon, J. A. and McMahon, A. P. (1993). Wnt-3a regulates somite and tailbud in the mouse embryo. *Genes Dev* **8**, 174-189.
Thermes, V., Candal, E., Alunni, A., Serin, G., Bourrat, F. and Joly, J.-S. (2006). Medaka simplet (FAM53B) belongs to a family of novel vertebrate genes controlling cell proliferation. *Development* **133**, 1881-1890.
Tian, Q., Feetham, M. C., Tao, W. A., He, X. C., Li, L., Aebersold, R. and Hood, L. (2004). Proteomic analysis identifies that 14-3-3z interacts with β-catenin and facilitates its activation by Akt. *Proc. Natl. Acad. Sci. USA* **101**, 15370-15375.
Valenta, T., Hausmann, G. and Basler, K. (2012). The many faces and functions of β-catenin. *EMBO J.* **31**, 2714-2736.
van der Flier, L. G., Haegebarth, A., Stange, D. E., van de Wetering, M. and Clevers, H. (2009). OLFM4 is a robust marker for stem cells in human intestine and marks a subset of colorectal cancer cells. *Gastroenterology* **137**, 15-17.
van Es, J. H., Haegebarth, A., Kujala, P., Itzkovitz, S., Koo, B.-K., Boj, S. F., Korving, J., van den Born, M., van Oudenaarden, A. and Robine, S. et al. (2012). A critical role for the Wnt effector TCF4 in adult intestinal homeostatic self-renewal. *Mol. Cell. Biol.* **32**, 1918-1927.
Vleminckx, K., Kemler, R. and Hecht, A. (1999). The c-terminal transactivation domain of β-catenin is necessary and sufficient for signaling by the LEF-1/β-catenin complex in *Xenopus laevis*. *Mech. Dev.* **81**, 65-74.
Weidinger, G., Thorpe, C. J., Wuennenberg-Stapleton, K., Ngai, J. and Moon, R. T. (2005). The Sp1-related transcription factors sp5 and sp5-like act downstream of Wnt/β-catenin signaling in mesoderm and neuroectoderm patterning. *Curr. Biol.* **15**, 489-500.
White, P. H., Farkas, D. R., McFadden, E. E. and Chapman, D. L. (2003). Defective somite patterning in mouse embryos with reduced levels of Tbx6. *Development* **130**, 1681-1690.
Wieschens, N. and Fagotto, F. (2001). CRM1- and Ran-independent nuclear export of β-catenin. *Curr. Biol.* **11**, 18-28.
Yokoya, F., Imamoto, N., Tachibana, T. and Yoneda, Y. (1999). beta-catenin can be transported into the nucleus in a Ran-unassisted manner. *Mol. Biol. Cell* **10**, 1119-1131.
Zhang, N., Wei, P., Gong, A., Chiu, W.-T., Lee, H.-T., Colman, H., Huang, H., Xue, J., Liu, M. and Wang, Y. et al. (2011). FoxM1 promotes β-catenin nuclear localization and controls Wnt target-gene expression and glioma tumorigenesis. *Cancer Cell* **20**, 427-442.
Zhou, S., Fujimuro, M., Hsieh, J. J.-D., Chen, L. and Hayward, S. D. (2000a). A role for SKIP in EBNA2 activation of CBF1-repressed promoters. *J. Virol.* **74**, 1939-1947.
Zhou, S., Fujimuro, M., Hsieh, J. J.-D., Chen, L., Miyamoto, A., Weinmaster, G. and Hayward, S. D. (2000b). SKIP, a CBF1-associated protein, interacts with the Ankyrin repeat domain of NotchIC to facilitate NotchIC function. *Mol. Cell. Biol.* **20**, 2400-2410.

Supplementary Materials

Title: Simplet/Fam53b (Smp) regulates Wnt signal transduction by inducing -catenin nuclear localization

Supplemental Materials and methods

Generation of zebrafish Smp antibody

The *smp* open reading frame with a deletion of the N-terminal at amino acid 119 was PCR-amplified and subcloning into the pET28 expression plasmid with an N-terminal His-tag. The plasmid was overexpressed by 0.4 mM IPTG to logarithmically growing E.coli Rosetta cultures, in LB-liquid medium for 3h at 30°C shaking at 250rpm. The cells were pelleted, suspended in NiNta buffer (25mM Tris pH 8.0, 250mM imidazole) supplemented with 5 mM imidazole, then lysed with Emulsiflex C5 (Avestin). Cell debris was removed by centrifugation (1h, 20000g), and protein was bound by NiNta beads (Qiagen). After washing of the beads, the His-tagged Smp fragment was eluted by increasing the imidazole concentration to 250mM. Aggregates were removed by size exclusion chromatography with an S200 column on an Aekta Purifier 10 HPLC system (both GE Healthcare) and PBS buffer. The identity of the purified Smp-fragment was confirmed by Mass-Spec analysis after tryptic digest of the respective protein band from a Coomassie-stained SDS-page gel on an Ultraflex TOF/TOF MALDI Spectrometer (Bruker Daltonik). Rabbits were immunized by injecting 4x 100µg of the purified antigen at 4 successive time points with Freund's adjuvent (1rst immunization with complete, 3 boost immunizations supplemented with the incomplete adjuvant). Specific antibodies were purified from the serum of the rabbit exhibiting the most prominent immune response by an affinity chromatography with purified Smp covalently coupled to a 1ml NHS-sepharose column.

Supplementary Figures

Figure S1: *smp* expression during embryonic development of zebrafish, Related to Figure 1. (A) Sequence comparison between human SMP/FAM53B and FAM53A and C, genes most closely related to Smp/Fam53b: sequence identities are 31% between B and A and 33% between B and C as shown by the conserved amino acids highlighted grey. The black lines indicate the two homology regions in the SMP/FAM53B protein described in this paper. (B) Immunohistochemistry staining for zebrafish Smp shows the presence of the maternal protein in the 8-cell embryo. (C) Immunohistochemistry for Smp at 16-cell stage also detects the presence of the protein. (D) Immunohistochemistry for Smp at 90% epiboly. Lettered boxes indicate location of panels E-G. (E-G) Enlarged images of anterior (E), ventral (F) and dorsal (G) sides of a stained zebrafish embryo at 90% epiboly shows broad expression of Smp protein primarily in the nuclei. Scale bars equal 50 μm (A-D) and 15 μm (E-G).

Figure S2: Characterisation of *smp* morpholinos, Related to Figure 1.(A) 94% of the embryos injected with the mismatch morpholino control for *smp* did not show a noticeable phenotype. (B) Knockdown of *smp* produced a majority of embryos lacking posterior structures, 31% that showed somites of different sizes, 6% that partially developed up to the start of somitogenesis and 6% that dead before somitogenesis. (C-E) Immunohistochemistry for zebrafish Smp in zebrafish embryos using the rabbit anti-zebrafish Smp (zSmp) polyclonal antibody and DAPI staining on mismatch *smp* control injected (C), antisense *smp* ATG morphant (D) and antisense *smp* splice site morphant embryos (E). (C'-D') Immunostainings without DAPI staining. (F) Graph of the measurements of the staining levels of staining by the rabbit anti-zSmp polyclonal antibody of each injected morpholino group. (G) Expression of maternally loaded protein at different stages of development and effect on protein expression after morpholino knockdown (MM) Mismatch, (ATG) ATG morpholino, (Splice) Splice-site morpholino. (H) Quantitation of maternal protein expression

profiles. (I) 7xTCF-mCherry activity at 95% epiboly after injection of GFP mRNA in the one-cell embryo. (J) 7xTCF-XLa.Siam:nlsmCherry activity in *smp* morphant. (K) 7xTCF-XLa.Siam:nlsmCherry activity after co-injection of *smp* mRNA with *smp* morpholino. (L) 24 hour zebrafish embryos with fluorescein-labeled mismatch morpholino for *smp* show no developmental phenotype. (M) Knockdown of *smp* with a fluorescein-labeled morpholino shows severe axis anterior-posterior axis defects. (N) Rescue of knockdown phenotype when *smp* mRNA is co-injected with *smp* antisense morpholino. (O) Graph depicts quantitative assessment of the anterior-posterior axis phenotype by *smp* mRNA. Numbers in the lower left corners in panels (I-K) indicate the number of embryos with the depicted expression patterns to the total number of embryos. Scale bars are 50 μm (I-K) and 300 μm (L-N).

Figure S3: Loss of *smp* activity does not affect Bmp, Nodal or Fgf signaling, Related to Figures 1,4. (A) *bmp2* expression in the marginal cells and the tailbud (insert) of mismatch-morpholino controls. (B) *bmp2* expression in *smp* morphants (Antisense) shows similar expression as controls at tailbud stage. (C) *bmp4* at the tailbud stage is located in the posterior tailbud. (D) *bmp4* expression in *smp* morphants is similar to controls. (E) *bmp7* expressed throughout the tailbud-staged embryo of mismatch controls. (F) *smp* morphants show similar *bmp7* expression. (G) qRT-PCR comparing the relative levels of Np63 expression between MM control and *smp* morphants. (H) Dorsal view of *ndr2* (*nodal related 2*) expression in the prechordal plate of control embryos at tailbud stage. (I) Dorsal view *ndr2* expression in *smp* morphants. (J) Lateral view of *goosecoid* (*gsc*) expression in controls at tailbud stage. (J') Dorsal view of *gsc* in controls. (K) Lateral view of *gsc* expression in *smp* morphants. (K') Dorsal view of *gsc* expression in *smp* morphants. (L) Dorsal view of *floating head* (*flh*) expression the prechordal plate of controls. (M) Dorsal view of *flh* expression in *smp* morphants. (N) Lateral view of *fgf8a* expression in controls show expression in midbrain-hindbrain boudary, and the mesendoderm of the tailbud. (N') Dorsal view of *fgf8a* expression

in midbrain-hindbrain of controls. (N'') Posterior view of *fgf8a* expression in tailbud of controls. (O) Lateral view of *fgf8a* expression in *smp* morphants. (O') Dorsal view of *fgf8a* expression in *smp* morphants. (O'') Posterior view of *fgf8a* expression in *smp* morphants. (P) Lateral view of *spry4* expression in controls showing midbrain-hindbrain expression and posterior expression. (P') Dorsal view of *spry4* expression in midbrain-hindbrain of controls. (P'') Posterior view of *spry4* expression in controls. (Q) Lateral view of *spry4* expression in *smp* morphants. (Q') Dorsal view of *spry4* expression *smp* morphants. (Q'') Posterior view of *spry4* expression in *smp* morphants. Lateral views: A-F, J, K, N-Q; elsewhere dorsal (H, I, L, M), anterior (N'-Q') or tailbud (N''-Q'') views. Numbers in the lower left corners in panels indicate the number of embryos with the depicted expression patterns to the total number of embryos. Scale bars: 100 μm (A-K,L-N,O,P,Q) and 50 μm elsewhere. Numbers below the Western blot bands indicate relative normalized abundance values.

Figure S4: Altered *cyp26a1* expression in *smp* morphants, Related to Figure 1. (A) *raldh2* expression in the paraxial mesoderm of mismatch controls at tailbud (A) and 2-somite stage (A´) embryos. (B) *raldh2* expression in *smp* morphants at tailbud (B) and 2-somite stage (B'). (C) *cyp26a1* in the margin and the presumptive brain of controls at 95% epiboly. (D) *smp* morphants have similar expression at the same stage. (E) At tailbud stage, controls had *cyp26a1* expression in the anterior pole. (F) *smp* morphants showed expansion of *cyp26a1* expression. (G) *cyp26a1* expression (blue) and 7xTCF-XLa.Siam:nlsmCherry reporter expression (red) in controls at 95% epiboly. (H) *cyp26a1* expression does not change at 95% epiboly in antisense-morphant embryos, while mCherry expression (Wnt signaling) is reduced. (I) *cyp26a1* expression at 95% epiboly in non-transgenic embryos after heat shock at 60% epiboly. (J) Expanded expression of *cyp26a1* at 95% epiboly in embryos harboring the hsp70:*dkk-1*-GFP transgene after heat shock at 60% epiboly. Numbers in the lower left corners in panels indicate the number of embryos with the depicted expression patterns to the total number of embryos. Scale bars: 100 m.

Figure S5: Convergent extension movements are not affected by knockdown of *smp*, Related to Figure 1. (A) *wnt5b* expression in the marginal zone of mismatch control embryos. (B) Similar expression of *wnt5b* in *smp* morphant (antisense) embryos. (C) *wnt11* expression in the body axis of mismatch controls. (D) *smp* morphants show similar expression of *wnt11* in the body axis. (E) Mismatch-control embryos were injected with CMTPX cell tracker dye into the upper marginal zone at 50% epiboly as shown by lateral view. (E') Dorsal view of a mismatch-control embryo showing labeled cells throughout the embryonic body axis. (F) *smp* morphant embryos (lateral view) were similarly injected with CMTPX cell tracker dye at 50% epiboly. (F') Dorsal view of CMTPX-positive cells align at the midline and cluster at the anterior region at tailbud stage similar to the mismatch control embryos. (G) Expression of *no tail* (*ntl*) (black arrows) in the posterior and *calpthesin L* (*hgg*) (white arrows) in the anterior of the mismatch control embryos. (H) Expression of *ntl* and *hgg* in *smp* morphants is similar to controls. Scale bars in A-F' are 100 μm.

Figure S6: Gastrulation markers at tailbud stage are unaffected by loss of *smp*, Related to Figure 1. (A) Mismatch-morpholino-control embryos show *dlx3b* expression in the neuroectoderm. (B) *dlx3b* expression is similar in *smp* morphants (Antisense). (C) *cassanova/sox32* (*cas/sox32*) is observed in developing endoderm in mismatch controls. (D) *smp* morphants display similar (*cas/sox32*) expression. (E) *tbx16* expression in the axial and paraxial mesoderm of control embryos. (F) *smp* morphants display similar *tbx16* expression. (G) *myod* staining in control embryos shows expression in the adaxial of the paraxial mesoderm. (H) *smp* morphants show similar *myod* expression. (I) Double staining for H3P and *dlx3b*. (J) Double staining for H3P and *dlx3b* in *smp* morphants show decrease in the number of H3P and *dlx3b* expression. (K) Double staining for H3P and *tbx16* expression in controls. (L) Double staining for H3P and *tbx16* in *smp* morphants. (M) Graph of the number of H3P-positive cells overlapping with confocal planes containing *dlx3b* expression. (N)

Graph showing number of H3P-positive cells that overlap with confocal planes showing *tbx16* expression. (O) Lateral view of *shh* expression in the developing prechordal plate of controls. (O') Dorsal view of *shh* expression in control embryos. (P) Lateral view of *shh* expression in *smp* morphants show expression along the length of the AP axis. (P') Dorsal view of *shh* expression in *smp* morphants shows that that its expression is wider than *shh* expression controls. (Q) Lateral view of *twist2* expression in the developing prechordal mesoderm in controls. (Q') Dorsal view of *twist2* expression in prechordal plate of control embryos. (R) *twist2* expression in *smp* morphants. (R') Dorsal view of *twist2* in *smp* morphants. (S) Dorsal view of early *ntl* expression in the developing prechordal plate. (T) Dorsal view of *ntl* expression in *smp* morphants. (U) Dorsal view of expression of *foxa2* in prechordal plate of controls. (V) Dorsal view of *foxa2* expression in *smp* morphants. (W) Measurements of the lateral dimensions of the prechordal plate genes show slightly increased dimensions of the prechordal plate in *smp* morphants and that this alteration is temporary based on measurements of the dimensions of *shh* expression at 5 somite embryos. Numbers in the lower left corners in panels indicate the number of embryos with the depicted expression patterns to the total number of embryos. Scale bars: 50 μm (A,B,E,F,I-L), 100 μm (C,D,O-T), 250 μm (G, H, O'-R',U',V').

Figure S7: Loss of Wnt activity not due to defects in cell proliferation, Related to Figure 1. (A) Immunostaining for histone-3 phosphorylation (H3P) in MM-control embryos (mismatch) at 95% epiboly. (B) H3P staining is reduced in same-staged *smp* morphants (antisense). (C) H3P staining is decreased in embryos treated with hydroxyurea (HU) and aphidicolin (AC). (D) Graph indicates the relative mitotic indices of mismatch controls (black), *smp* morphant (grey) and HU/AC-treated embryos (white) through development. (E) 7xTCF-siam:mCherry activity in control embryos. (F) Activity of the Wnt-reporter in *smp* morphants. (G) Wnt-reporter activity in HU/AC-treated embryos. Scale bars equal 100 μm. "***" is $p < 0.005$.

Figure S8: Apoptosis is not responsible for the loss of posterior structures in *smp* morphants, Related to Figure 1. (A) Measurement of TUNEL-positive cells in mismatch (MM-MO) control embryos and *smp* morphants (AS-MO). (B) Measurement of Annexin-V-positive cells in MM-control embryos and *smp* morphants. (C) Graph showing the effect of p53 morpholino knockdown in MM-control and and *smp*-morphant embryos. (D) A 10-hour-old *p53*-knockdown larva shows no effect on the expression of the 7xTCF:mCherry reporter. (E) *smp-p53* double knockdown shows that loss of p53 does not restore the expression of the Wnt-dependent reporter in embryos lacking *smp*. (F) A *smp* morphant at 10 hours post fertilization shows loss of report expression. Scale bars equal 100 μm.

Figure S9: Smp knockdown does not affect ligand-induced activation of Wnt signaling, Related to Figure 2. (A) Expression of *wnt3* in mismatch-control (MM-MO) embryos. (B) Expression of *wnt3* in *smp* morphants (AS-MO). (C) Expressison of *wnt8* in MM-control embryos. Inset shows posterior expression. (D) Expression of *wnt8* in *smp* morphants. Inset shows posterior expression. (E) Western blots of phospho-Lrp6 from MM controls and *smp* morphants. Values indicate relative abundance. Numbers in the lower left corners in panels indicate the number of embryos with the depicted expression patterns to the total number of embryos. Scale bars equal 100 μm.

Figure S10: Smp knockdown in vivo results in the loss of Smp protein and redistribution of -catenin to the cytoplasm, Related to Figure 2. (A) Immunoblots of subcellular fractionation between nuclear and cytoplasmic lysates for -catenin, PCNA (nuclear marker), GAPDH (cytoplasmic) and -tubulin (loading control). (B) Immunoblot for zebrafish Smp protein (zSmp) in embryos injected with a mismatch morpholinos (mm-mo) and antisense morpholinos (as-mo) against *smp* mRNA either at the translational start site

(ATG) or the first exon-intron boundary (Splice). (C) Immunoblot for -tubulin served as loading control.

Figure S11: Smp synergizes with multiple members of the -catenin-dependent Wnt signal transduction cascade, Related Figure 2. (A) Transfection of pBAR luciferase reporter in HEK293T cells in the absence or presence of either zebrafish *smp* or -catenin. (B) Synergy of zebrafish *smp* with different components of the Wnt signal transduction cascade in luciferase assays when cotransfected in HEK293T cells. (C) Graded increase of co-transfected *smp* expression plasmid (100ng, 150 ng, 200ng, 250ng, 300ng) proportionally increases the activity of the pBAR-luciferase promoter.

Figure S12: Smp expression and subcellular distribution is not regulated by Wnt signaling, Related to Figure 2. (A) Graph shows expression levels of *smp* mRNA by qRT-PCR from 9 hpf zebrafish embryos of non-transgenic (non-TG) and transgenic lines: Tg[wnt8-GFP], Tg[axin-GFP] and Tg[dkk1-GFP] after heat shock. (B) Graph shows fold GFP expression levels from each heat shocked non-transgenic and transgenic line at 9 hpf. (C) Graph shows expression levels of smp by qRT-PCR from each non-transgenic and transgenic line at 12 hpf. (D) Graph shows fold GFP expression levels from each heat shocked transgenic line at 12 hpf. (E-H) Immunocytochemistry for Smp (E,F) and -catenin (G,H) shows that smp nuclear localization is not enriched by addition of Wnt3a to the cells. (I,J) DAPI staining for untreated and Wnt3a-treated cells, respectively. All fish lines were heat shocked at shield stage using the same method in Experimental Procedures.

Figure S13: Quantitation of in vivo reporter response to regulation of smp function. (A) Graph of measured mCherry expression of Tg[7xTCF-siam:mCherry] transgenic embryos after injection of GFP, stabilized -catenin, stabilized -catenin with full length Smp or mutant

Smp harboring a dysfunctional NLS. **(B)** Representative western blot for mCherry. **(C)** Representative blot for gamma tubulin as loading control.

Figure S14: Reduction of SMP protein by transfection of Smp siRNA, Related to Figure 4. (A) Immunohistochemistry for SMP in mouse intestine (black arrowheads). **(B)** *in situ* hybridization for the -catenin-dependent gene Olfm4 (black arrowheads).

Figure S15: Reduction of SMP protein by transfection of Smp siRNA, Related to Figure 4. (A) Western blot of immnoprecipitation pull down of -catenin with different mutants of the Smp protein. **(B)** Western blot of antibody to the endogenous SMP protein in control siRNA- and SMP siRNA-transfected HEK293T cells. **(C)** Same blot samples probed with alpha-tubulin antibody. **(D)** Measurement of fold expression detected from Western blot of siRNA knockdown experiment. **(E-L)** Expression of GFP fused to the C-terminal of Smp. **(E)** Smp-GFP alone and **(F)** Bright field image of (E). **(G)** Smp-GFP in cells transfected with control siRNA. **(H)** bright field of (G). **(I)** SMP-GFP fluorescence in the cells transfected with 100 nM siRNA to Smp. **(K)** SMP-GFP in cells transfected with 200 nM of siRNA to Smp. **(M)** Lucifierase reporter assay for control -catenin, Smp-FL and Smp delta homology region (I). **(N)** Fluorescence recovery curves after photobleaching mCherry- -catenin in nucleus of cell transfected either with GFP or Smp. Scale bars equal 100 μm.

Supplementary References

Brand, Michael, Granato, Michael and Nüsslein-Volhard, Christiane (2002) Keeping and raising zebrafish. in Ralf Dahm and Christiane Nüsslein-Volhard (eds.) *Zebrafish: A Practical Approach*. Oxford: Oxford University Press.

Kimmel, Charles B., Warga, Rachel M. and Schilling, Thomas F. (1990) 'Origin and Organization of the Zebrafish Fate Map', *Development* 108: 581-594.

Kizil_Fig S1

A

```
FAM53B MVMILRRSLINQGADSGAHRTF-IPELHTPKMSQGPTLLSCGI-MENDRWRDLDRKCPLQIDQPSASIWECLPEKCQ--DGSLWHQEAVTACAVTSLIKDLNINDHNGN
FAM53A MVTLITEKLQNQSLDDLTRRACEAGPYSAEKLNKSGHLFPLEISVDKSPWKALRGGWPTG-SQAASGPFSVGPHGVSHTEGLKWQLESPGPMDVGHF---LDLHDSTGP
              10        20        30        40        50        60        70        80        90        100

FAM53C PPAPPSKRHCRSLSVPVDLSRWQPVWRPAPSKLWTPIKHRGNAGGGGPQ-VPQQ--S--PPKRVSSLRFLQAPSASSQCAPAHRPYSPPFFSLALAQDSAQPCATSPQSGSWESDAES
FAM53B PSAPPSKRQCRSLSFSDEMSSCRTSWRPLGSKVWTPVEKRRCYSGGSVQ-RYSNGVS--PMQRSSS--FSLPARANGLSSPCHQSSLHHRFG-------GQPCQGAPGSAPCGQAGDS
FAM53A PAAPPTKRHCRSLSEPEELARCRSPWRPGSSKVWTPISKRRCNSGGSATLQCCSGVGNPTLQGTLV  PGLPRRPVSPAGPT--SPLTPRPA-------SASSGFVDGSEGSTSSGPP
          110       120       130       140       150       160       170       180       190       200       210

FAM53C LSPCPPQ----RRFSLSPSLGPQASRFL------PSARSSPASSPELPWRPRGLRNLPRSRSQPCDLDARKTGVKRRHEEDCRRLRPSLDFDKMNQ-KPYSGGLCCLQETAREEGSNVSP
FAM53B W-SPDPHPVGGGRLDLQRSLSCSHEQFSFPEYCPPSANSTPASTPELARRSSGL---ARSRSQPCVLNDKKIGVKRRRPDEVQEQRPSLDLAKMAQNCQTFSSLSCLNMGVDDHSSQ-SP
FAM53A WLSTGPCPFSS-----RRRLSLSQEHLVDTGACLPSASSTPTSTPELGRHH-GL---LRCRSQPCVLDGRRVRRKRRREEDARWTRPSLDFLKMTRTLKNSKSLCSLDYEDDEDDTQ-EK
          220       230       240       250       260       270       280       290       300       310       320

FAM53B FALVSSTRSWTALLSASSPGGRTPAGTP-VPEPVPHSFDDQFTCQEDLSCDESDGCSLDEDCCRKGDPATSWRDRGACTNSLCSLD-GELDIEQIENN
FAM53A -TLVSSPCNSQGLV-----GIITPSSSPRIPRPGPDSPSIWASGEPEANPGEG-GSS--------GDP-SDWDSAGE--EGIFPLDHGDLDLEQIENN
          330       340       350       360       370       380       390       400
```

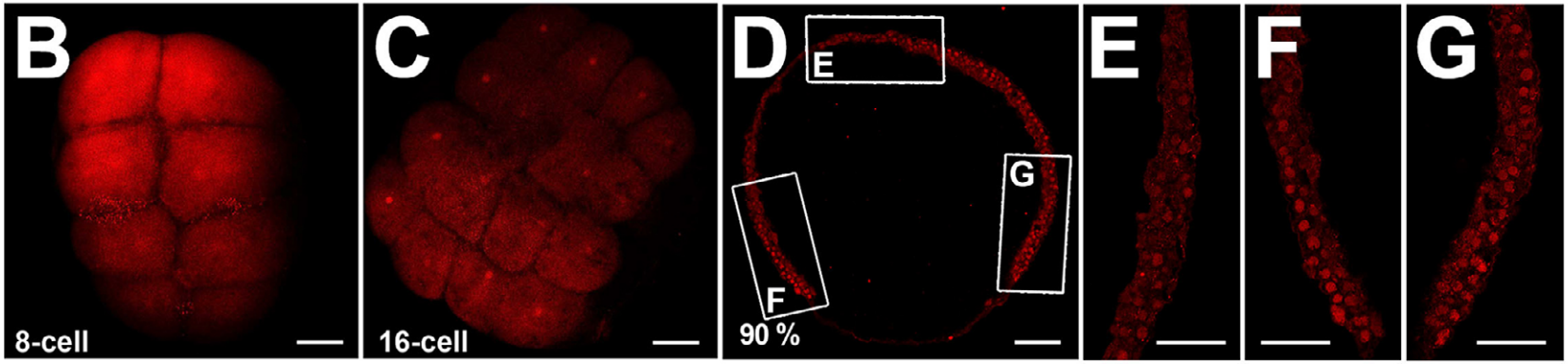

Kizil Fig S2

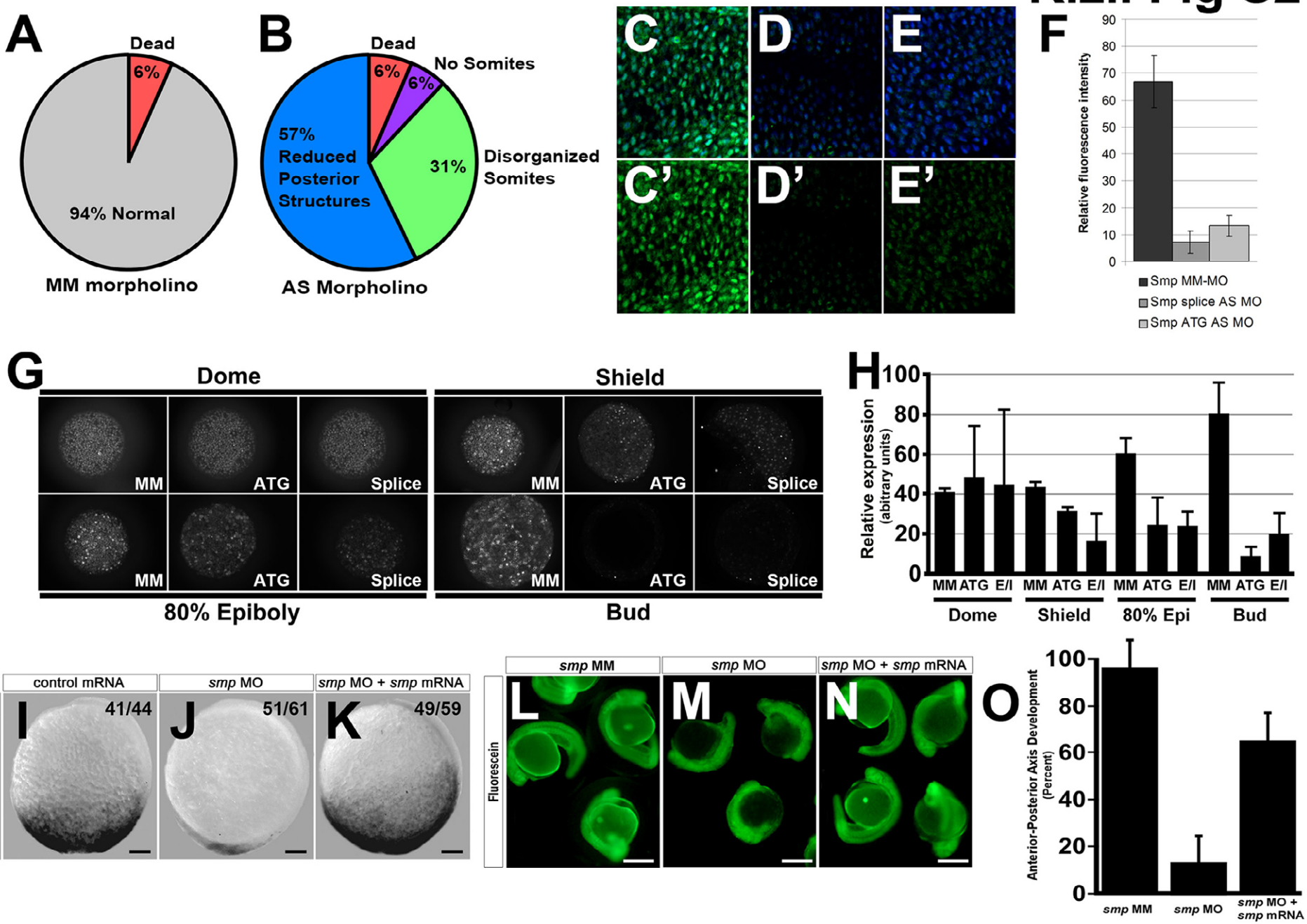
A
Dead
6%
94% Normal
MM morpholino
B
Dead
6%
No Somites
6%
57%
Reduced
Posterior
Structures
31%
Disorganized
Somites
AS Morpholino
C
D
E
C'
D'
E'
F
Relative fluorescence intensity
90
80
70
60
50
40
30
20
10
0
Smp MM-MO
Smp splice AS MO
Smp ATG AS MO
G
Dome
Shield
MM
ATG
Splice
80% Epiboly
Bud
H
Relative expression
(abitrary units)
100
80
60
40
20
0
MM ATG E/I
Dome
Shield
80% Epi
Bud
control mRNA
smp MO
smp MO + smp mRNA
mCherry
I
41/44
J
51/61
K
49/59
smp MM
smp MO
smp MO + smp mRNA
Fluorescein
L
M
N
O
Anterior-Posterior Axis Development
(Percent)
100
80
60
40
20
0
smp MM
smp MO
smp MO +
smp mRNA

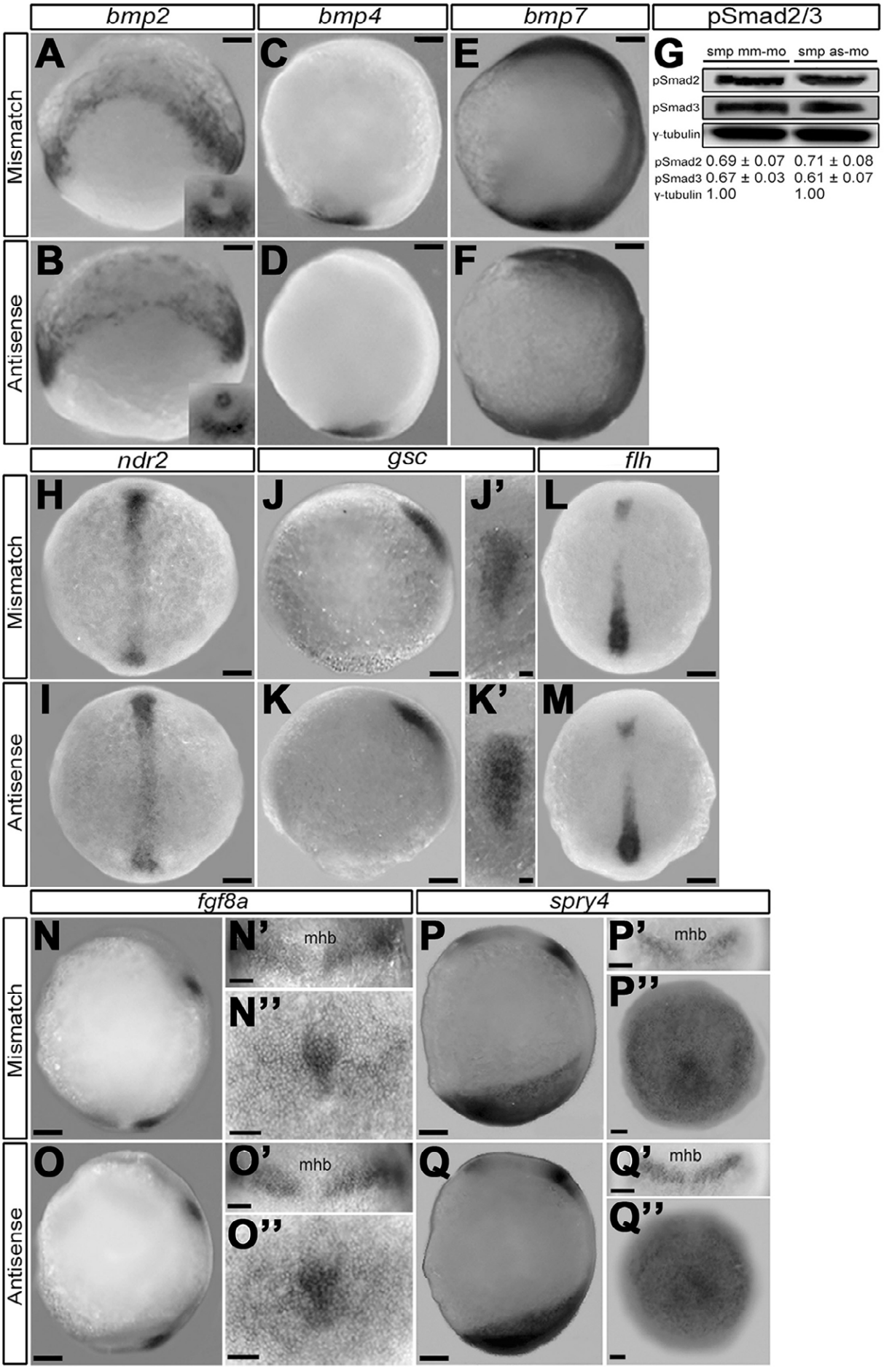
bmp2
bmp4
bmp7
pSmad2/3
Mismatch
Antisense
A
B
C
D
E
F
G
smp mm-mo
smp as-mo
pSmad2
pSmad3
γ-tubulin
pSmad2 0.69 ± 0.07 0.71 ± 0.08
pSmad3 0.67 ± 0.03 0.61 ± 0.07
γ-tubulin 1.00 1.00
ndr2
gsc
flh
H
I
J
J'
K
K'
L
M
fgf8a
spry4
N
N'
N''
O
O'
O''
P
P'
P''
Q
Q'
Q''
mhb

KIzil_Fig. S3

Kizil_Fig S4

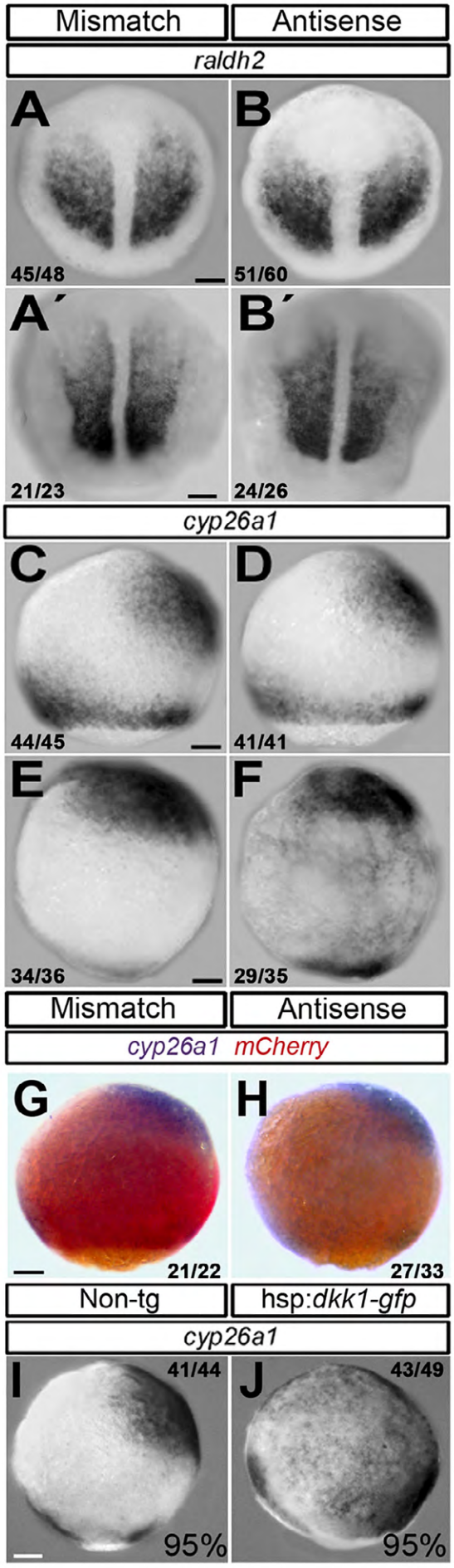
Mismatch
Antisense
raldh2
A
B
45/48
51/60
A´
B´
21/23
24/26
cyp26a1
C
D
44/45
41/41
E
F
34/36
29/35
Mismatch
Antisense
cyp26a1 mCherry
G
H
21/22
27/33
Non-tg
hsp:dkk1-gfp
cyp26a1
I
J
41/44
43/49
95%
95%

Kizil_Fig S5

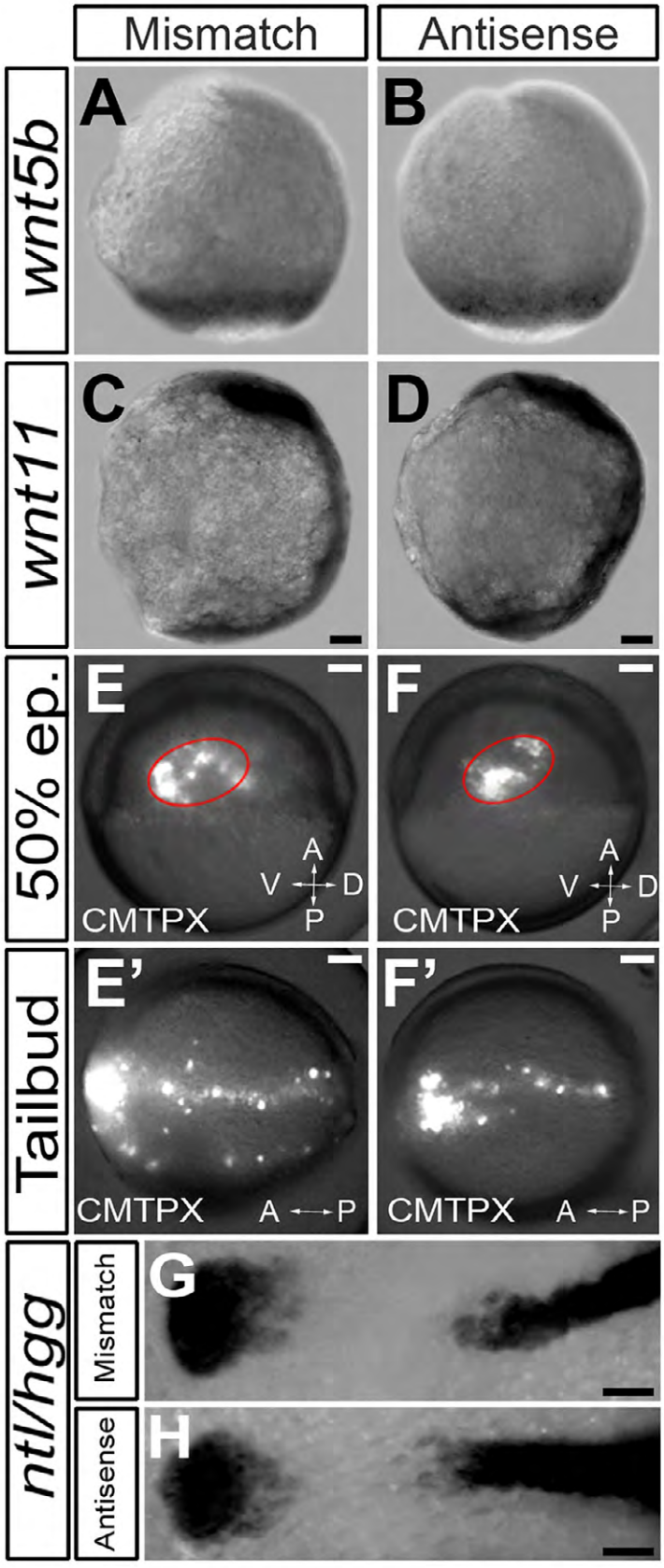
Mismatch
Antisense
wnt5b
A
B
wnt11
C
D
50% ep.
E
F
A
V
D
P
CMTPX
Tailbud
E'
F'
CMTPX
A
P
ntl/hgg
Mismatch
Antisense
G
H

Kizil_Fig S6

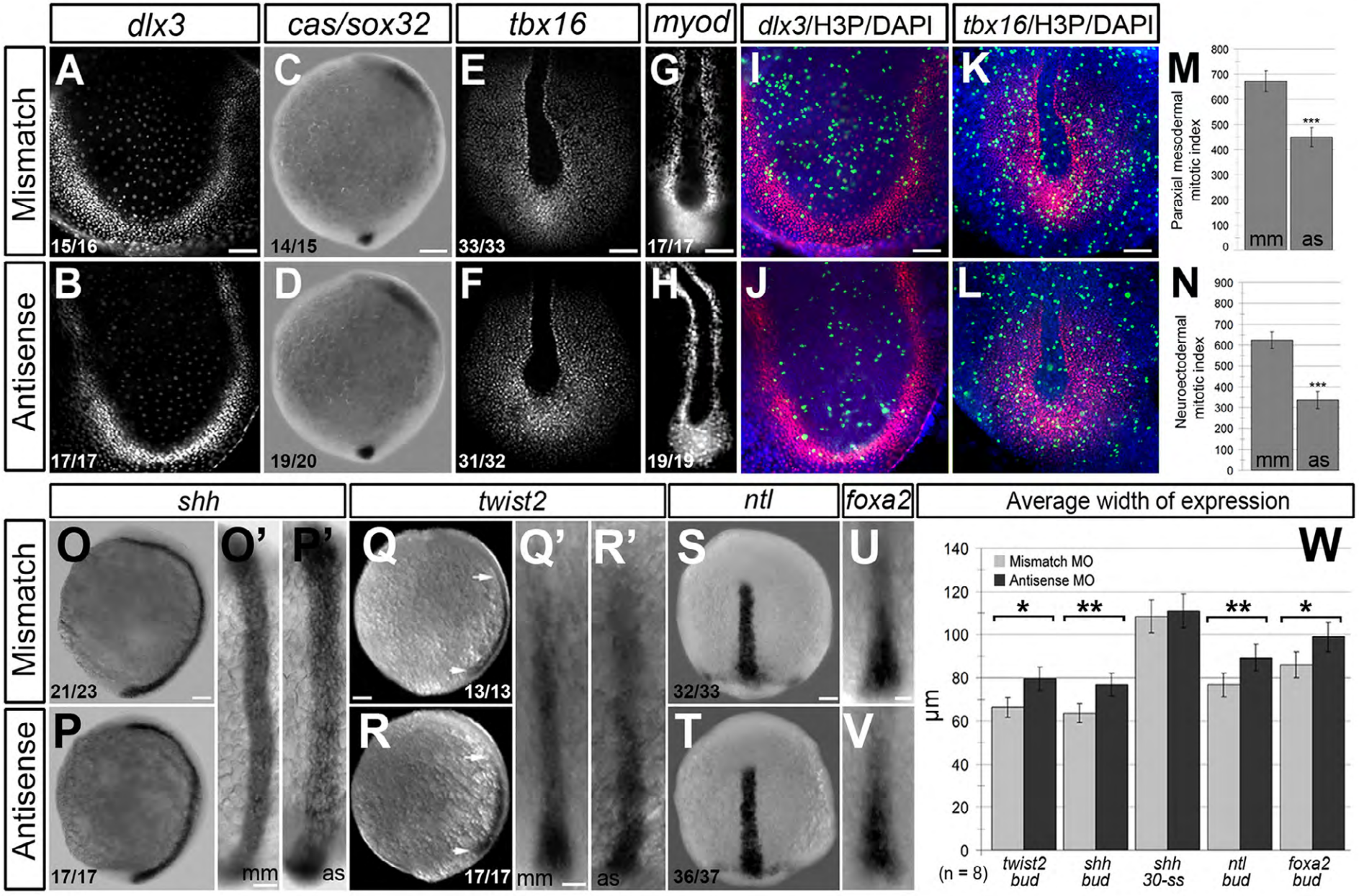
dlx3
cas/sox32
tbx16
myod
dlx3/H3P/DAPI
tbx16/H3P/DAPI
Mismatch
Antisense
A
B
C
D
E
F
G
H
I
J
K
L
15/16
17/17
14/15
19/20
33/33
31/32
17/17
19/19
M
Paraxial mesodermal mitotic index
mm
as
***
N
Neuroectodermal mitotic index
shh
twist2
ntl
foxa2
Average width of expression
O
O'
P'
Q
Q'
R'
S
U
P
R
T
V
21/23
17/17
13/13
17/17
32/33
36/37
W
Mismatch MO
Antisense MO
µm
(n = 8)
twist2 bud
shh bud
shh 30-ss
ntl bud
foxa2 bud

Kizil_Fig S7

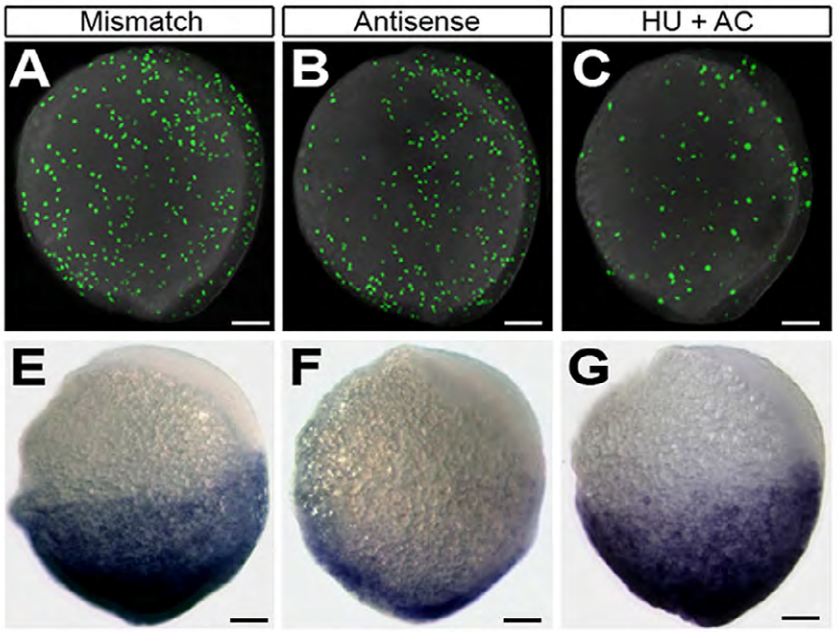
Mismatch
Antisense
HU + AC
A
B
C
E
F
G

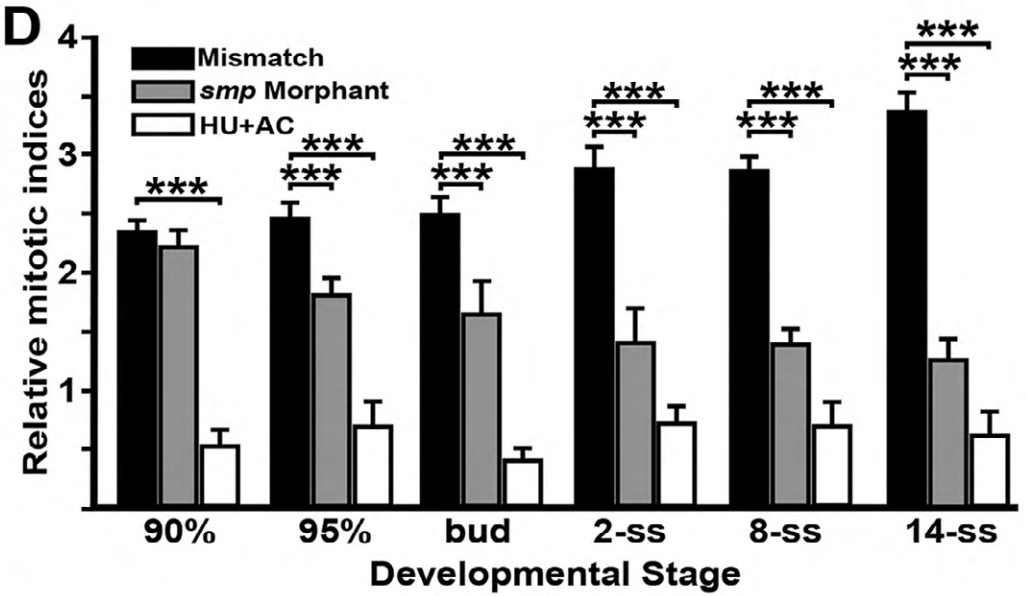
D
Mismatch
smp Morphant
HU+AC
Relative mitotic indices
1
2
3
4
***
90%
95%
bud
2-ss
8-ss
14-ss
Developmental Stage

Kizil_Fig S8

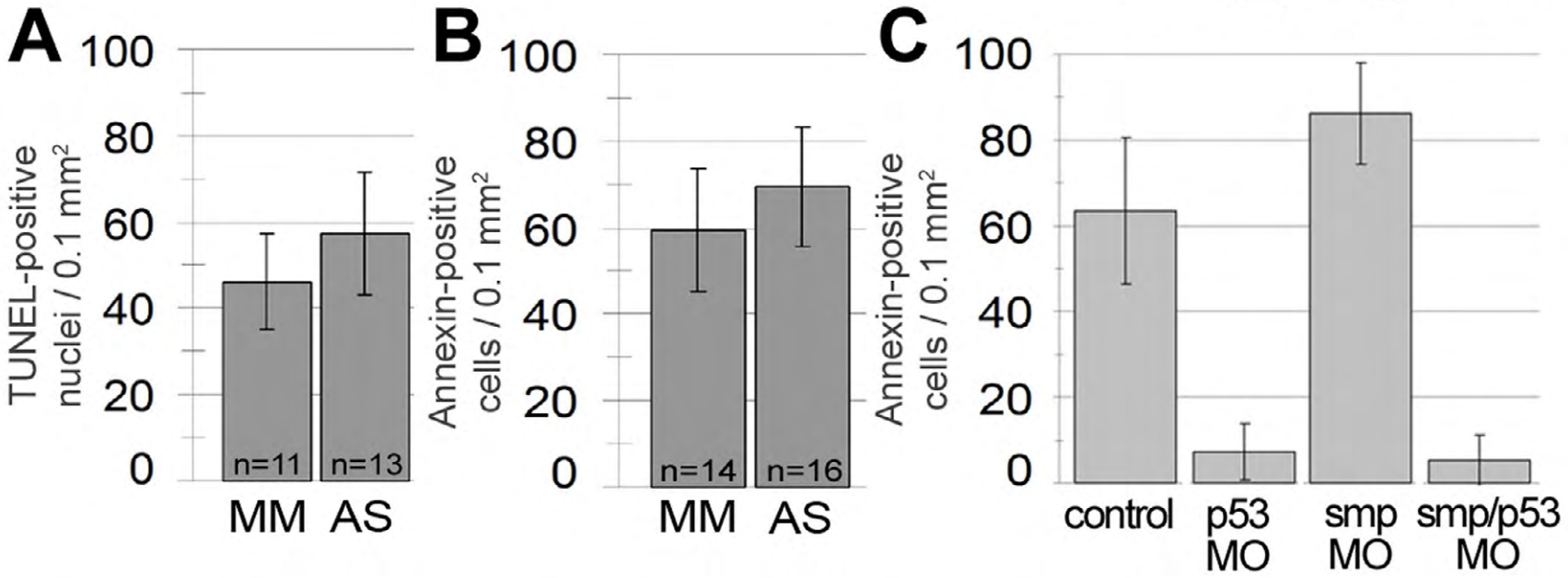
A
TUNEL-positive nuclei / 0.1 mm²
100
80
60
40
20
0
n=11
n=13
MM
AS
B
Annexin-positive cells / 0.1 mm²
100
80
60
40
20
0
n=14
n=16
MM
AS
C
Annexin-positive cells / 0.1 mm²
100
80
60
40
20
0
control
p53 MO
smp MO
smp/p53 MO

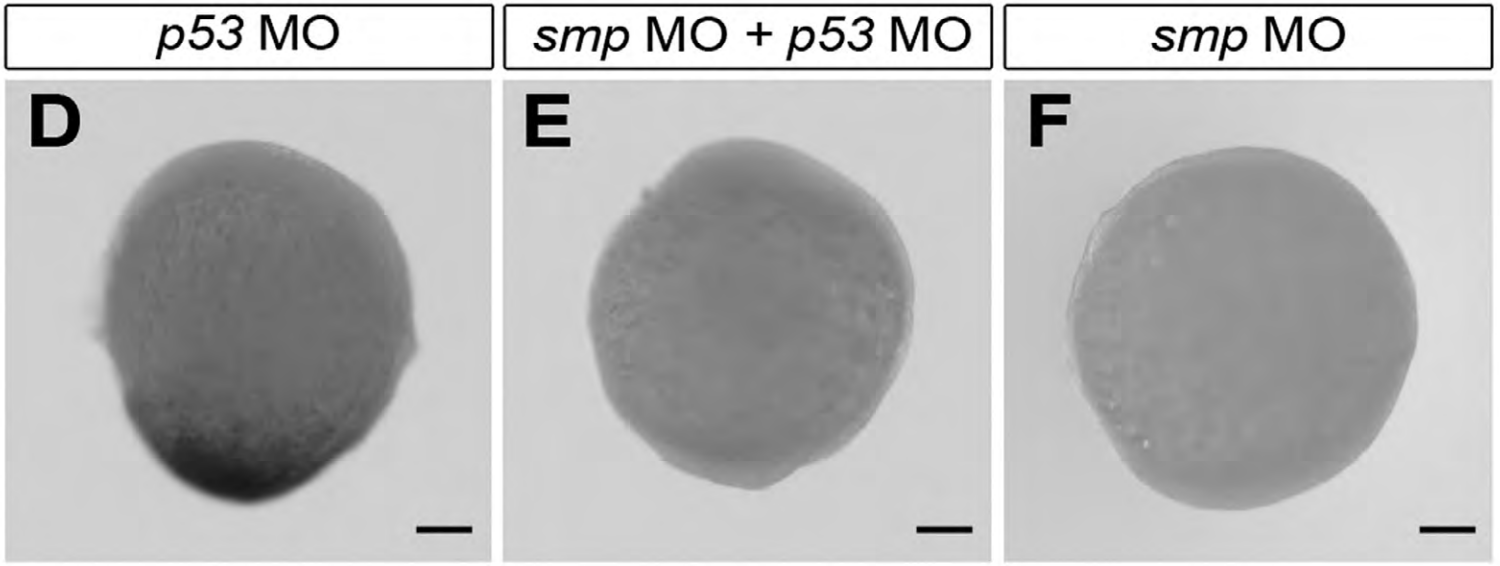
p53 MO
smp MO + p53 MO
smp MO
D
E
F

Kizil_Fig S9

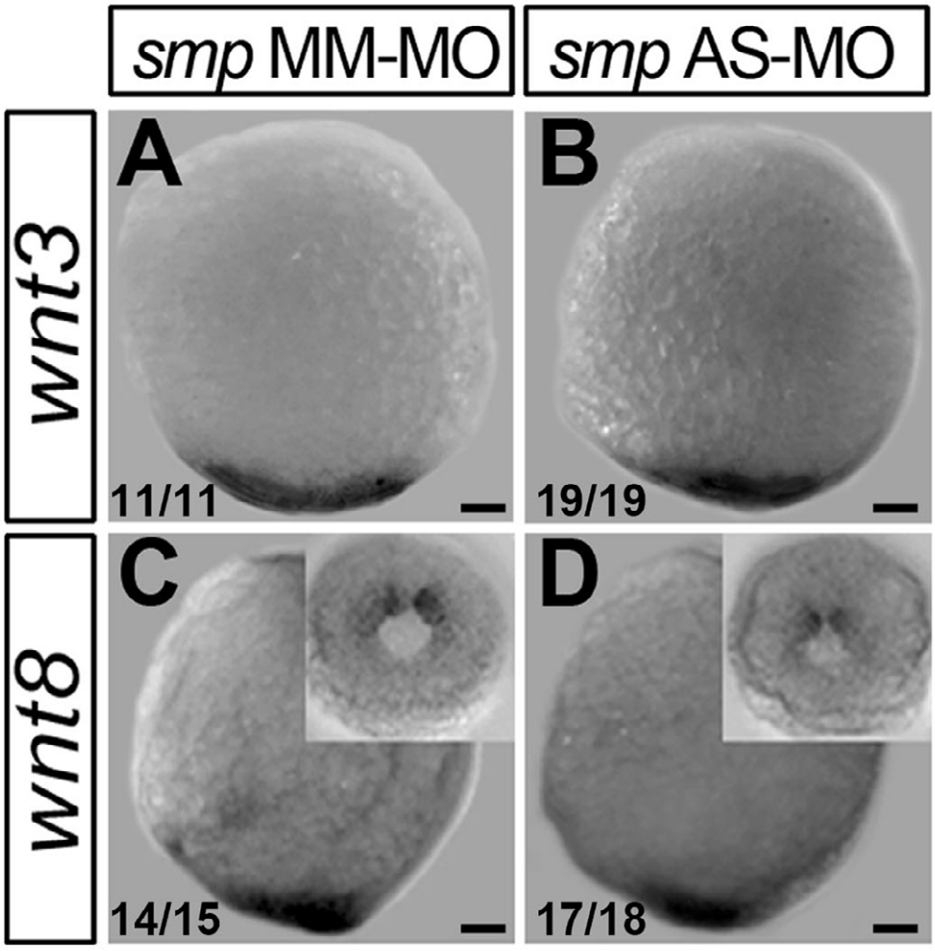
smp MM-MO
smp AS-MO
wnt3
wnt8
A
B
C
D
11/11
19/19
14/15
17/18

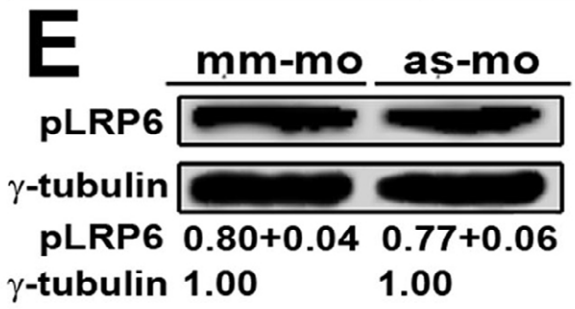
E
mm-mo
as-mo
pLRP6
γ-tubulin
pLRP6 0.80+0.04 0.77+0.06
γ-tubulin 1.00 1.00

Kizil_Figure S10

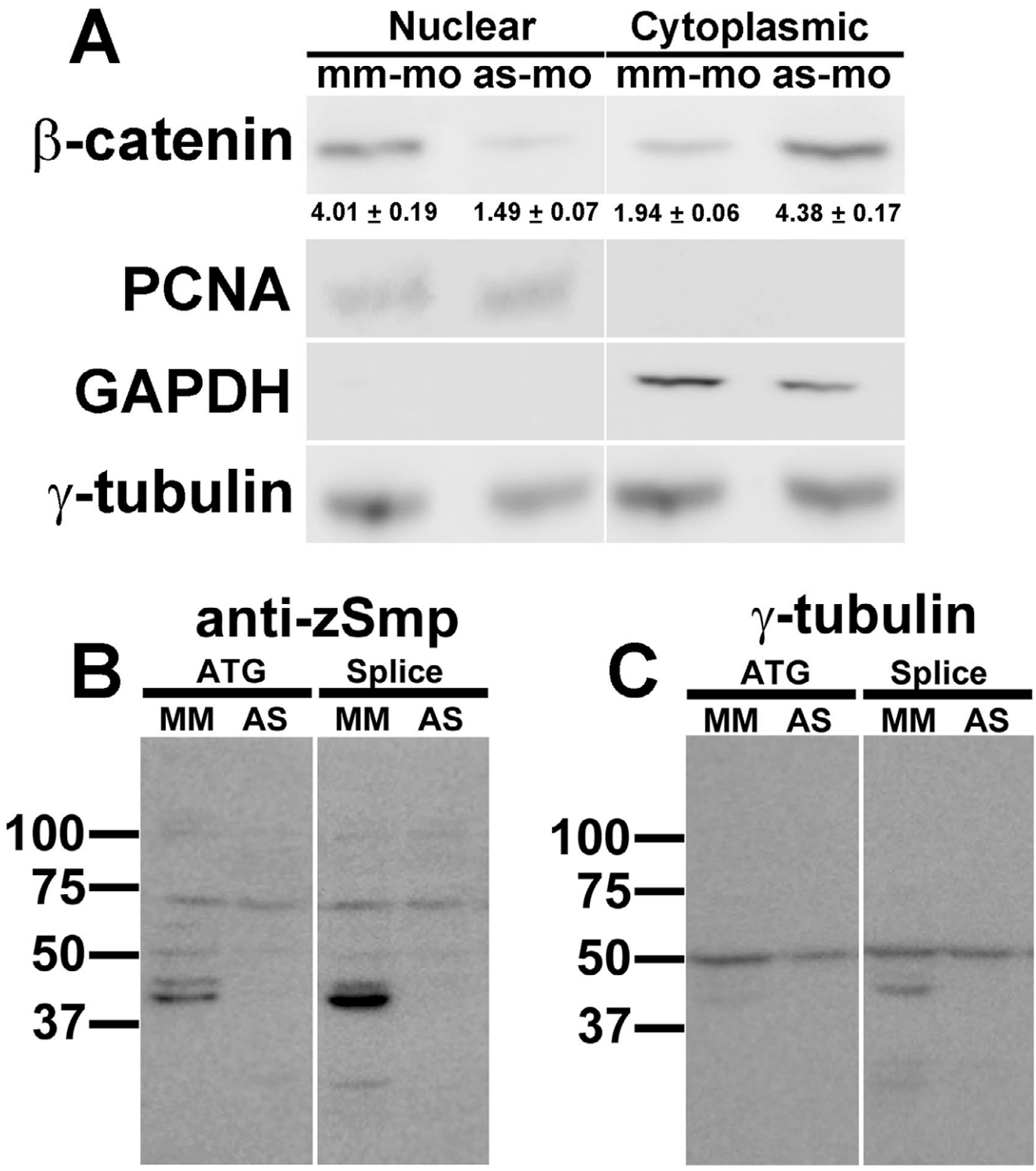

Kizil_Fig S11

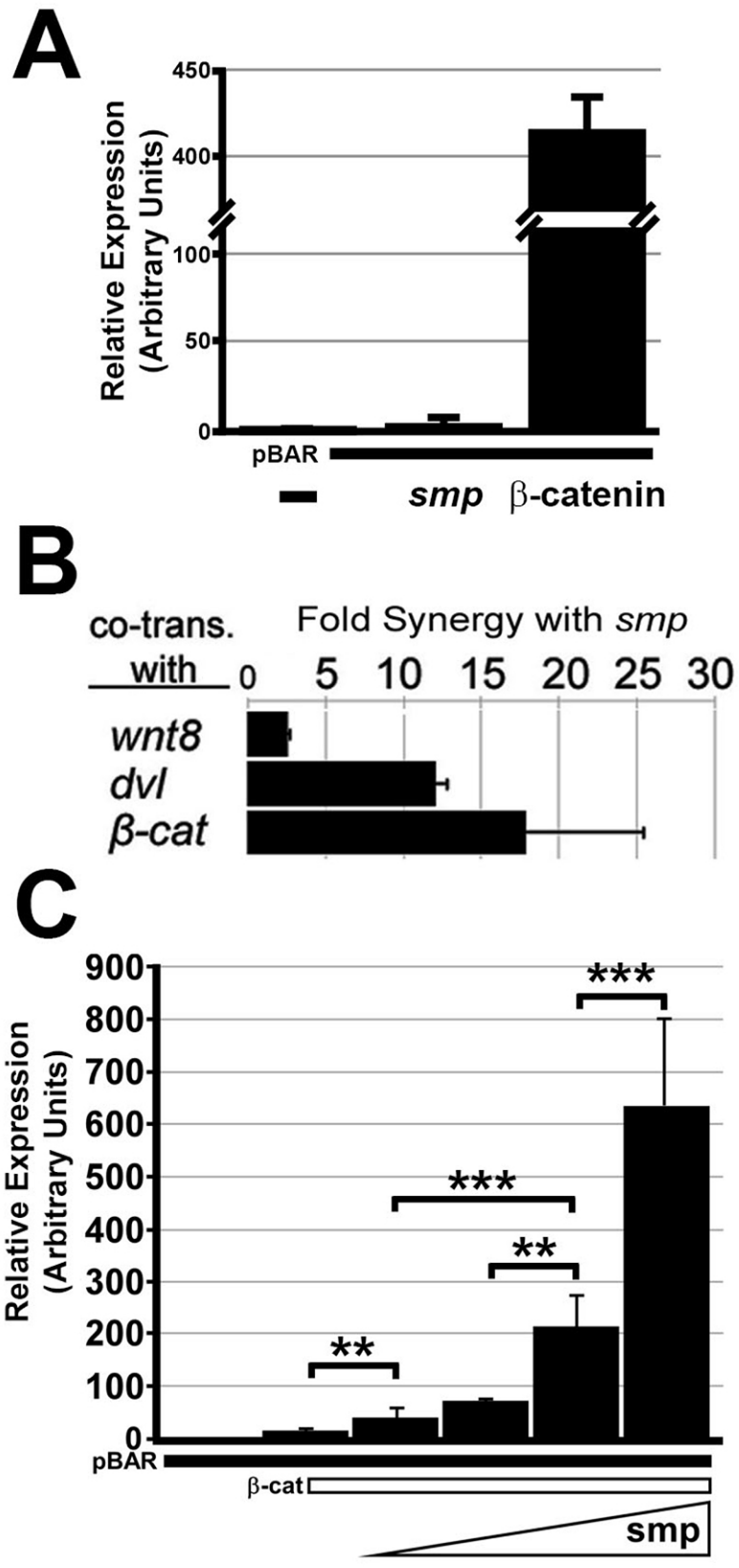

Kizil_Fig S12

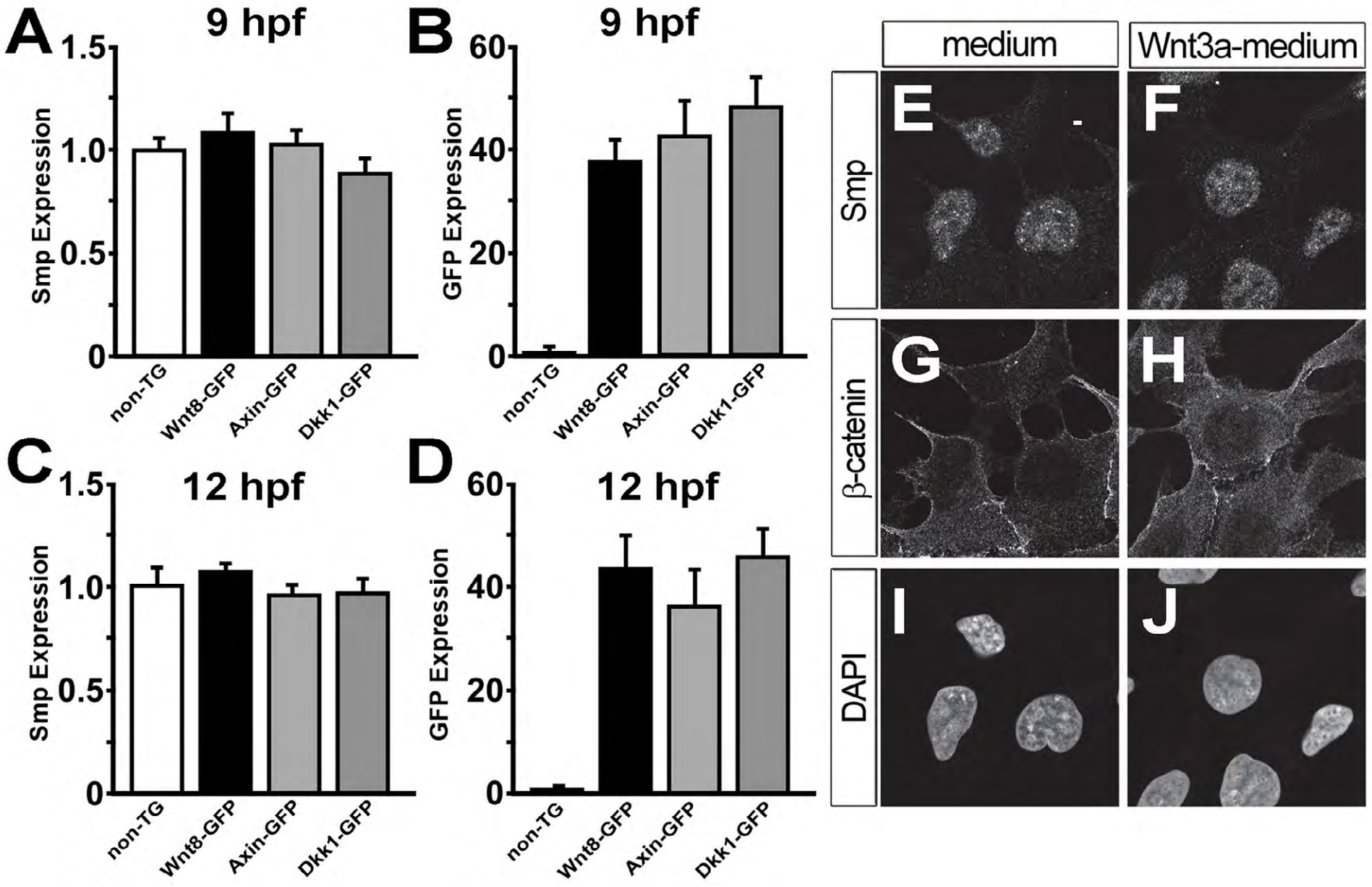

Kizil_Fig. S13

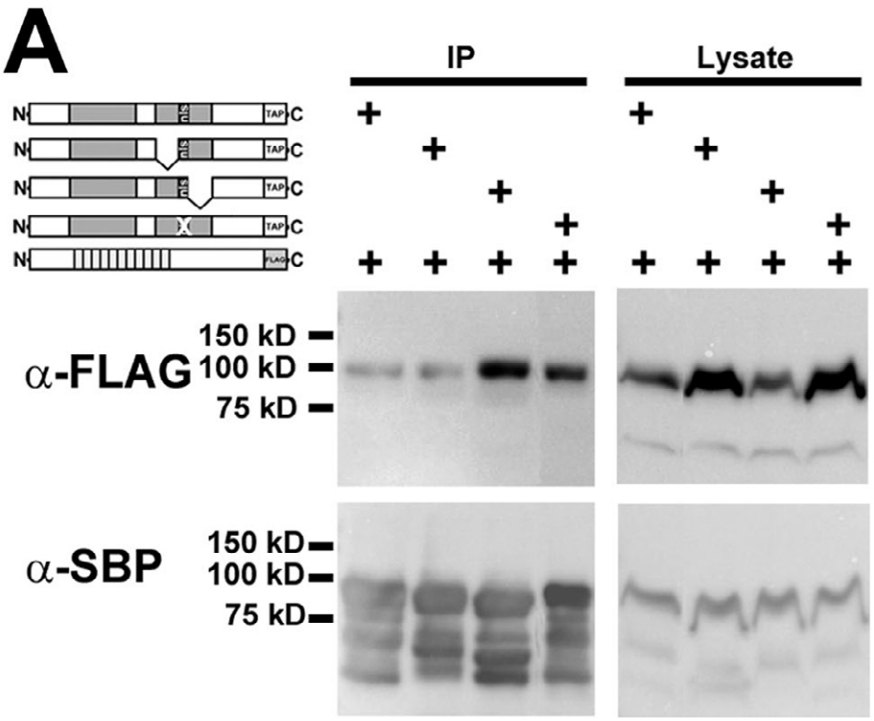

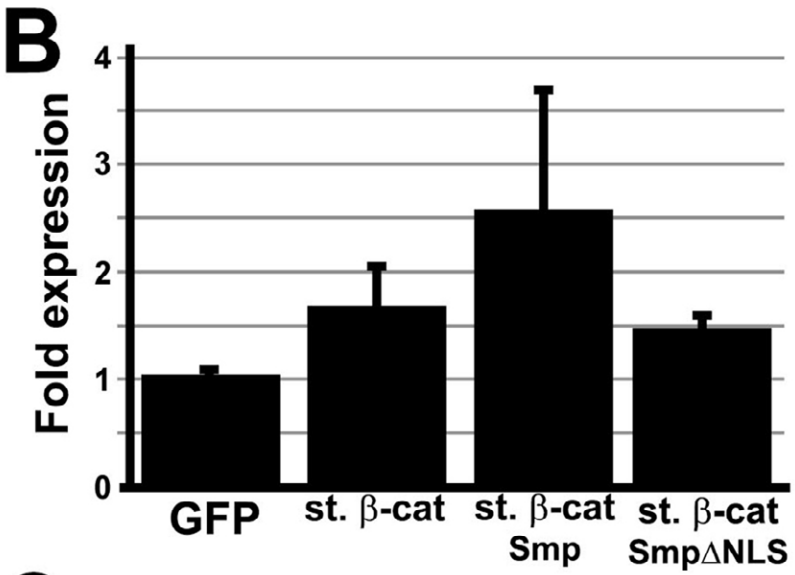

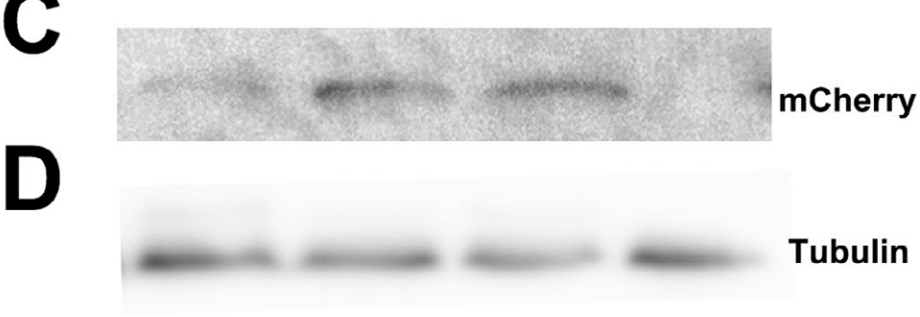

Kizil_Fig. S14

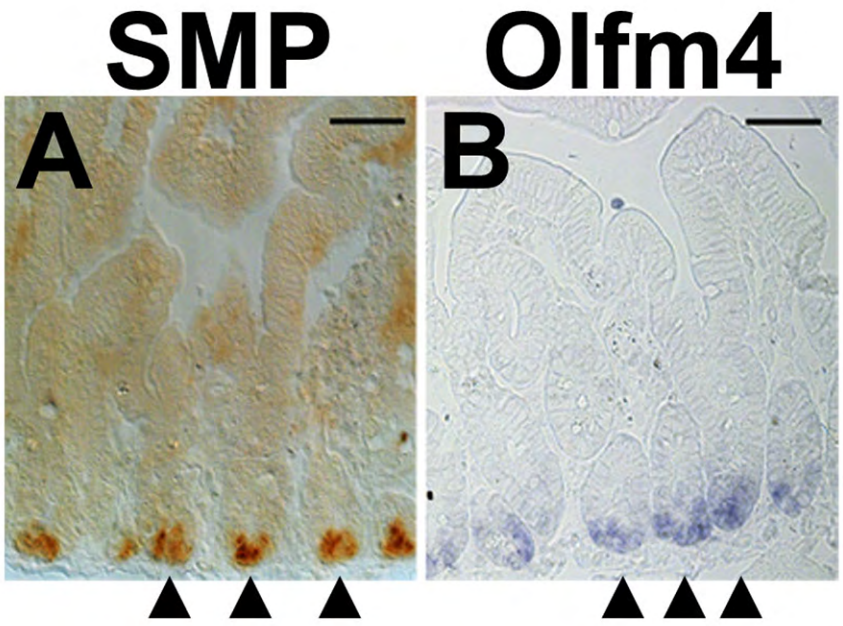

Kizil_Fig S15